capsule. After transplantation, nonfasting blood glucose level was monitored using samples from tail blood by Glutest PRO (Sanwa kagaku, Nagoya, Japan). Normoglycemia after transplantation was defined as two consecutive blood glucose levels below 200 mg/dl. Islet rejection after transplantation was defined when two consecutive blood glucose levels exceeded 200 mg/dl. At 1 week posttransplantation, the engrafted kidneys were excised to assess the survival of islet grafts by immunohistochemistry. Moreover, the beneficial effects of monotherapy with intraperitoneal sivelestat in recipient mice were assessed. Sivelestat was administered at 100 mg/kg/day for 1 day before transplantation and every day until 14 days after transplantation, as described previously (32). The recipient Balb c/A mice treated with sivelestat were divided at random into two experimental groups ($n=5$/group) to receive allogeneic islets isolated from C57BL/6J mice using ET-Kyoto or S-Kyoto solution.

Intraperitoneal Glucose Tolerance Test (IPGTT)

The IPGTT was performed at 1 week posttransplantation, using the method described previously (2,9,58). Mice ($n=3$/group) were fasted overnight and then injected intraperitoneally (IP) with 2 g glucose in saline/kg body weight. Untreated diabetic mice and nondiabetic wild-type mice were transplanted with saline as a control. Blood glucose levels were measured before injection and at 15, 60, and 120 min after injection.

Immunohistochemical Analysis

Immunohistochemical analysis was performed using the method described previously (36). The engrafted kidneys were excised, fixed in formalin, and embedded in paraffin. Tissue sections (2-μm thick) were placed in 0.3% H_2O_2/methanol to quench endogenous peroxidase activity and incubated with 5% bovine serum albumin (BSA)-PBS to block nonspecific reaction. The slides were incubated with rabbit anti-insulin polyclonal antibody (pAb, Santa Cruz Biotechnology, CA) to detect the transplanted islets. The sections were incubated with horseradish peroxidase (HRP)-conjugated secondary antibody (Bethyl Laboratories, Inc., Montgomery, TX) and then immunostaining was visualized with 0.02% DAB (Sigma-Aldrich) as the chromogen. After washing, the sections were counterstained with hematoxylin. Control tissue sections were prepared in a similar fashion, except no primary antibody was used.

Measurement of Proinflammatory Cytokines

The supernatant was collected after each step of islet isolation, including before warm digestion, at the end of warm digestion and after purification. Moreover, serum samples were collected from islet recipients at day 1 before transplantation and days 4, 7, 14, 21, 28 after transplantation. These samples were frozen immediately at −80°C until analysis. Proinflammatory cytokine (IL-2, IL-4, IL-6, IL-10, IL-17A, IFN-γ, TNF-α) levels in these samples were measured using the BD™ Cytometric Bead Array Mouse Th1/Th2/Th17 CBA kit (BD Biosciences, San Jose, CA) and analyzed on a FACS Calibur Flow cytometer (BD Immunocytometry).

Statistical Analysis

Values were expressed as mean±SD. Differences between groups were examined for statistical significance using the two-tailed unpaired Student's t test or one-way analysis of the variance (ANOVA) followed by Bonferroni's post hoc test when multiple comparisons were made. A value of $p<0.05$ denoted the presence of significant difference.

RESULTS

Direct Cytotoxicity of Neutrophil Elastase and Optimum Effective Concentration of Sivelestat

To assess the direct cytotoxicity of NE against isolated islets, LDH assay was performed at various concentrations of this enzyme. NE caused 43–48% killing at both 5 and 10 μg/ml. To prevent this killing, sivelestat was added to the culture medium at 2, 20, or 200 μM. The cytotoxicity induced by 10 μg/ml of NE could not be inhibited by sivelestat (Fig. 1A). However, the cytotoxicity induced by less than 5 μg/ml of NE was significantly abrogated by either 20 or 200 μM of sivelestat, but not by 2 μM of sivelestat (Fig. 1A).

To elect the optimum concentration of sivelestat for islet isolation, islet isolation was performed by the addition of various concentrations of sivelestat to the isolation solution (Fig. 1B). Islet yields using a high concentration of sivelestat (200 μM or 2 mM) were significantly lower than that with 20 μM of sivelestat. In contrast, no significant improvement in islet yield was observed by 2 μM of sivelestat isolation compared with that of the control group (ET-Kyoto isolation). These findings correlated with those from LDH assay, and thus, the following experiments were performed using 20 μM of sivelestat.

Activation of Neutrophils in Pancreas During Collagenase Digestion

Naphthol AS-D chloroacetate esterase staining was performed to demonstrate whether resident neutrophils in the pancreas tissue are activated by collagenase digestion. Many neutrophils were activated (red-brown staining) by collagenase digestion in islet isolation using both UW and ET-Kyoto solutions (Fig. 2A), but their number (cells/field) was significantly reduced by the addition of 20 μM of sivelestat in ET-Kyoto solution (UW: 10.2±1.1, S-UW: 6.8±0.4, ET-Kyoto: 9.2±1.3, S-Kyoto: 3.6±0.5) (UW, ET-Kyoto vs. S-Kyoto: $p<0.001$, S-UW vs. S-Kyoto:

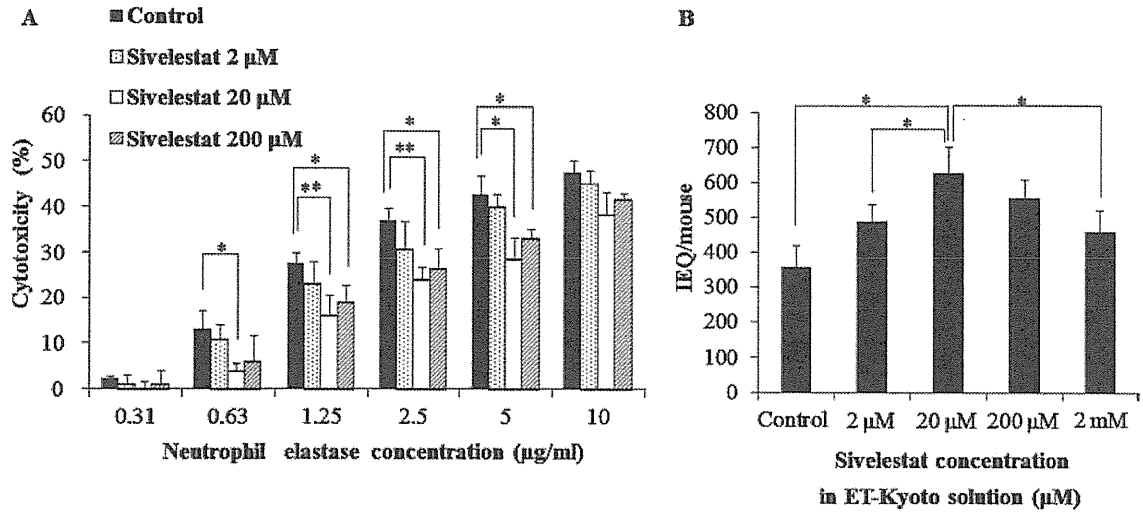

Figure 1. In vitro cytotoxicity assay of neutrophil elastase against islets and optimum concentration of sivelestat in ET-Kyoto solution. (A) The cytotoxicity of neutrophil elastase against islets and the inhibitory effects of sivelestat were assessed by lactate dehydrogenase (LDH) assay. Data are mean ± SD of three independent experiments; $*p<0.05$, $**p<0.01$. (B) Islet yields under various concentrations of sivelestat. Data are mean ± SD of three independent experiments; $*p<0.05$.

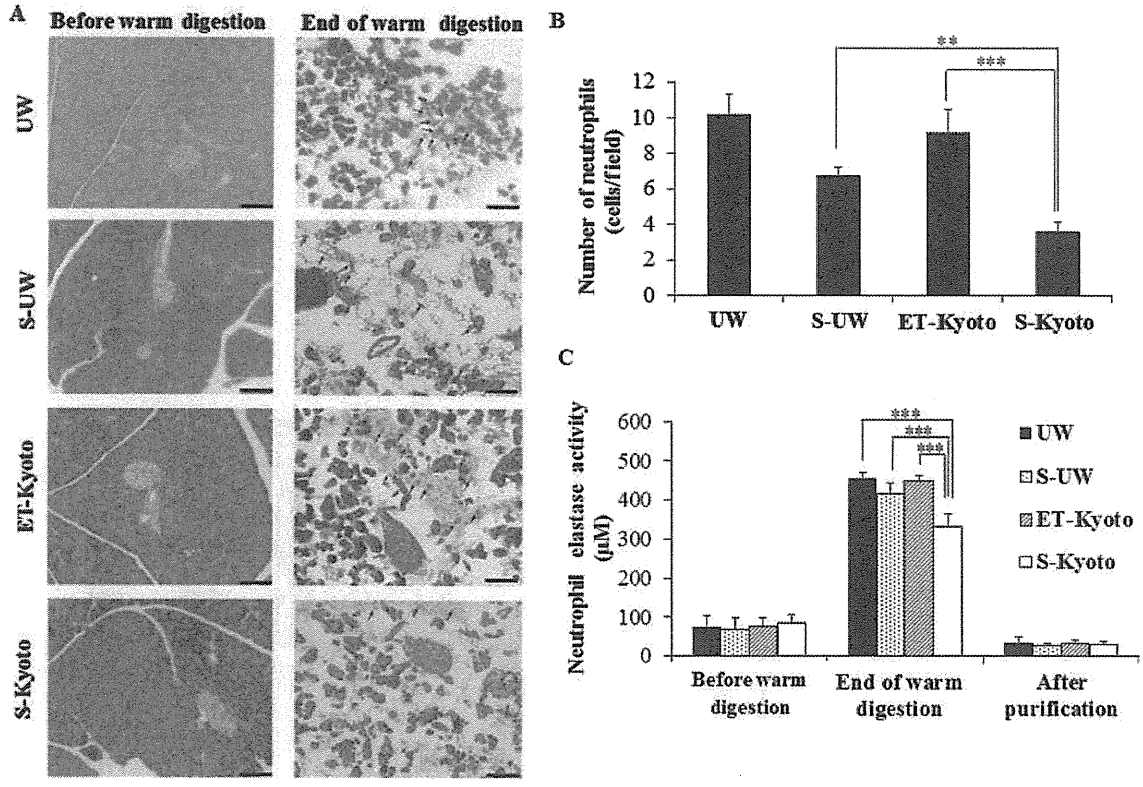

Figure 2. Accumulation of activated neutrophils in the pancreas and neutrophil elastase activity during islet isolation. (A) Representative histology of the pancreas before and at the end of warm digestion. Activated neutrophils are stained red-brown (black arrow) by naphthol AS-D chloroacetate esterase. Scale bars: 100 μm. (B) Number of activated neutrophils per field (original magnification: 100×) was counted under microscopy. Data are mean ± SD of five sections; $**p<0.01$, $***p<0.001$. (C) Neutrophil elastase activity in the supernatant during islet isolation measured at various time points of islet isolation (before warm digestion, at the end of warm digestion, after purification). Data are mean ± SD of five independent samples; $***p<0.001$. UW, University of Wisconsin solution.

$p<0.01$) (Fig. 2B). These results suggest a marked increase in enzyme activity by collagenase digestion in all types of isolation solutions (Fig. 2C). However, the enzyme activity was significantly suppressed in S-Kyoto islet isolation than those in other isolations (UW, S-UW, and ET-Kyoto isolation).

Sivelestat Suppresses Apoptosis in Islets After Warm Digestion During Islet Isolation

Many TUNEL-positive cells were identified in the islets at the end of warm digestion (Fig. 3A), whereas no such cells were detected before digestion (data not shown). Quantitative analysis indicated a significantly lower number of TUNEL-positive cells within the islets of the S-Kyoto group (6.6±1.5) compared with those of UW, S-UW, and ET-Kyoto groups (23.1±3.9, 20.8±5.0, and 15.3±2.6, respectively) ($p<0.001$, each) (Fig. 3B).

Improvement of Islet Yield Elicited by Islet Isolation With S-Kyoto Solution

To investigate the beneficial effects of sivelestat in islet isolation, islet isolations were performed using either UW or ET-Kyoto solution, with or without 20 μM of sivelestat. Islet yield, isolation index, and islet purity after purification were significantly improved by S-Kyoto islet isolation (Table 1). The recovery rate of purification was also significantly improved by S-Kyoto islet isolation, compared to those by other isolation solutions (UW: 55.8±10.4%, S-UW: 56.6±12.7%, ET-Kyoto: 56.6±4.6%, S-Kyoto: 76.0±5.2%). Based on the results of UW isolation groups (UW, S-UW), no beneficial effects of sivelestat were elicited under these islet isolation parameters. With regard to islet size distribution, the percentage of large islets (>150 nm in diameter) in the S-Kyoto group was markedly higher than that in other isolation groups (Fig. 4A).

To further examine the morphological changes in isolated islets, SEM was employed. As shown in Figure 4B, islets obtained from the UW groups (UW, S-UW) were poor, based on the irregular islet surface and detection of islet damage during the isolation procedure. Similarly, islets obtained from ET-Kyoto isolation had irregular shape. On the other hand, islets isolated by S-Kyoto solution were well preserved, with round and smooth surface.

Improvement of Islet Viability Elicited by Islet Isolation With S-Kyoto Solution

Next, we evaluated islet viability using fluorescence labeling with TMRE and 7-AAD (Fig. 5). In the UW groups (UW, S-UW), no significant difference was noted in islet viability assay using TMRE and 7-AAD between with or without sivelestat [UW ($n=5$) vs. S-UW ($n=5$) (60.0±5.6% vs. 63.3±4.4%, not significant)]. However,

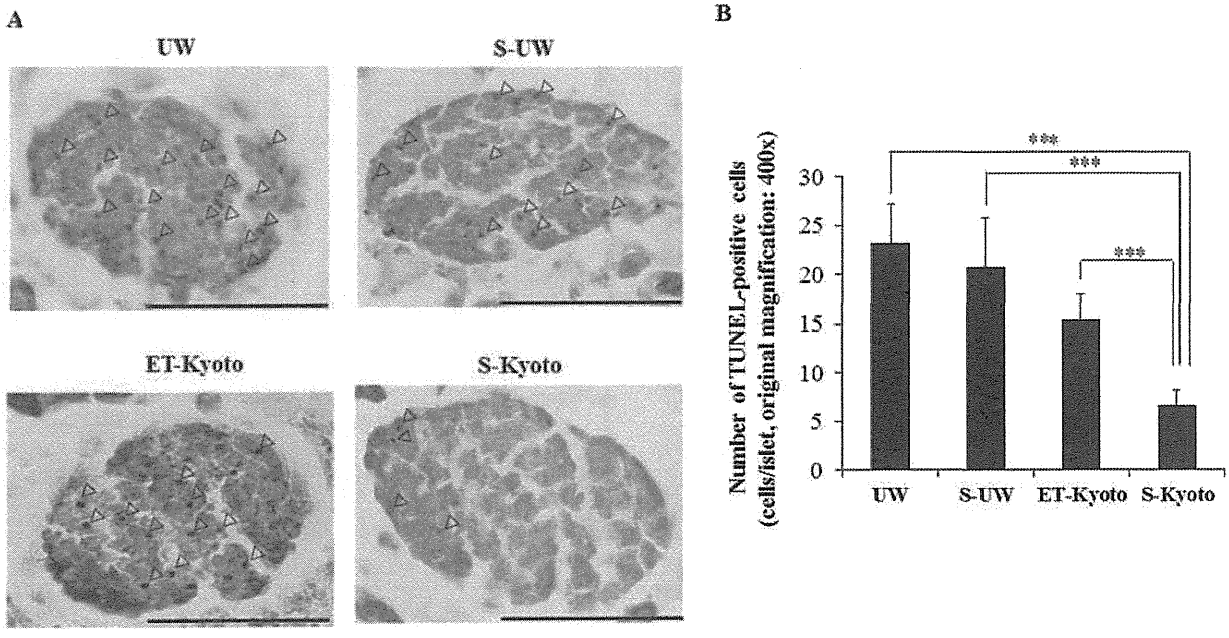

Figure 3. Assessment of apoptosis during islet isolation by TUNEL staining. (A) Representative histological sections of the islets at the end of warm digestion. Note the brown terminal deoxynucleotidyl transferase dUTP nick-end labeling (TUNEL)-stained apoptotic cells (arrowhead). Scale bars: 100 μm. (B) The density of TUNEL-positive cells (cells/islet) was determined under magnification of 400×. All experiments were done using each independent mouse. One mouse was used in each experiment ($n=1$). Data are mean±SD of five independent sections; ***$p<0.001$.

Table 1. Results of Islet Isolation According to the Isolation Solution

	UW	S-UW	ET-Kyoto	S-Kyoto
Islet count after purification (cells/mouse)	248±92*	270±121	280±86	332±74
IEQ after purification	243±68§	276±126¶	367±70*	651±52
Recovery rate of purification	55.8±10.4¶	56.6±12.7*	56.6±4.6*	76.0±5.2
Isolation index	1.18±0.21§	1.20±0.38¶	1.56±0.21*	2.05±0.17
Islet purity (%)	82.7±3.1§	84.0±2.2¶	87.3±2.7	91.3±1.9

Data are expressed as mean±SD of five independent experiments. *$p<0.05$, ¶$p<0.01$, §$p<0.001$, compared with S-Kyoto isolation solution. Islet count and purity were measured by the VH analyzer software. Isolation index was calculated as the ratio of IEQ to islet count. The recovery rate of purification (%)=IEQ after purification/IEQ before purification×100. IEQ, islet equivalents; UW, University of Wisconsin.

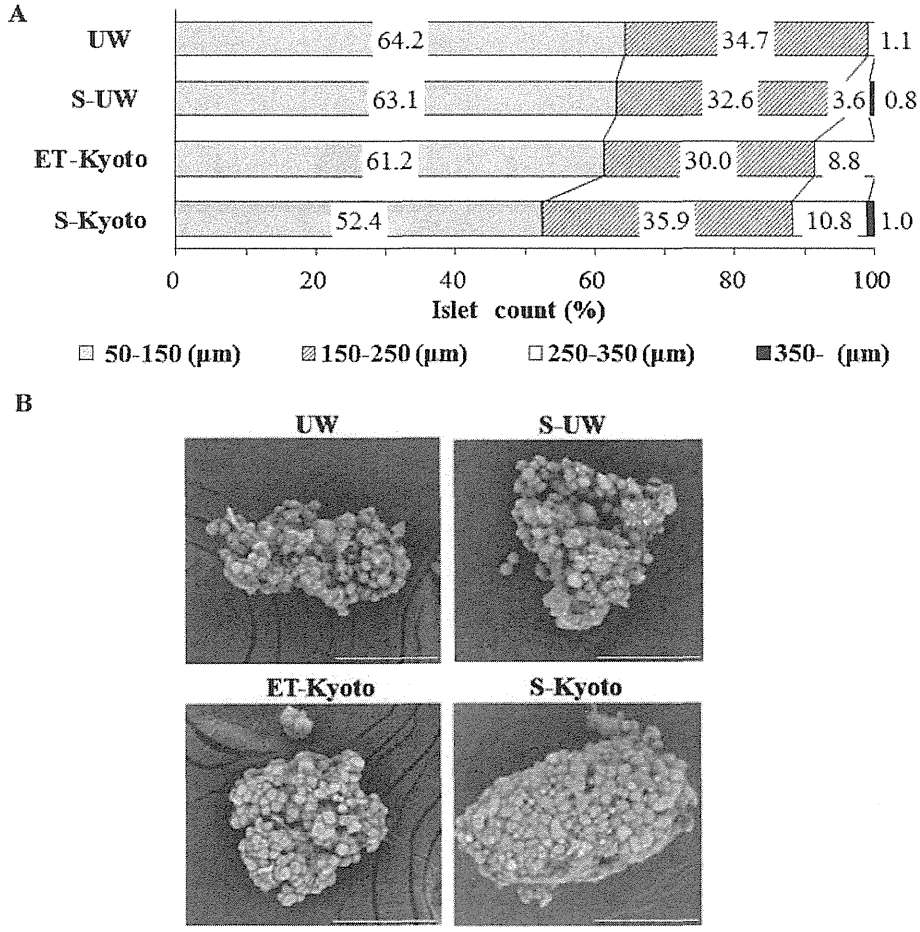

Figure 4. Results of islet isolation according to the type of isolation solution. (A) Size distribution for each diameter (50–150, 150–250, 250–350, 350– μm) of isolated islets assessed by using each isolation solution. All experiments were done using each independent mouse. One mouse was used in each experiment ($n=1$). Data are the mean percentage from five independent experiments. (B) Representative microscopic images of the islets immediately after isolation. The morphology of isolated islets was observed by scanning electron microscopy. Scale bars: 100 μm.

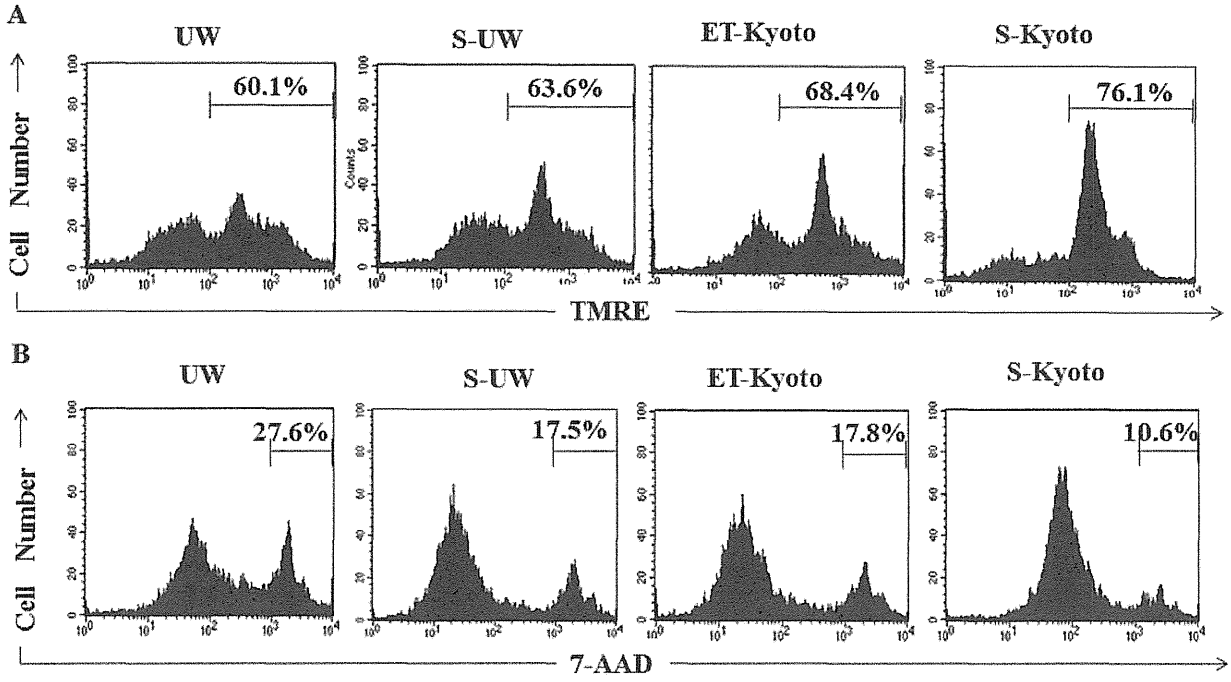

Figure 5. In vitro viability assay of isolated islets by TMRE and 7-AAD. (A) Representative flow cytometry analysis by tetramethyl rhodamine ethyl ester (TMRE) assay. (B) Representative flow cytometry analysis by 7-aminoactinomycin D (7-AAD). Percentage data represent percentages of cells with high fluorescence.

the percentage of dead cells, represented by 7-AAD-positive cells, was significantly reduced in S-UW isolation group [UW (n=5) vs. S-UW (n=5), 25.8±5.3% vs. 17.2±1.3%, p<0.05]. In contrast, the viability of islets isolated with S-Kyoto solution was significantly better relative to that of ET-Kyoto isolation [ET-Kyoto (n=5) vs. S-Kyoto (n=5), 67.0±1.2% vs. 75.4±2.0%, p<0.001]. Moreover, the percentage of dead cells in the S-Kyoto group was also lower compared with that in ET-Kyoto isolation [ET-Kyoto (n=5) vs. S-Kyoto (n=5), 18.6±2.2% vs. 11.6±2.4%, p<0.01]. Similar findings of islet viability were noted by MTS assay (Fig. 6A). The highest viability of fresh islets was noted with S-Kyoto solution [ET-Kyoto (n=5) vs. S-Kyoto (n=5), 0.172±0.013 vs. 0.206±0.026, p<0.05] (Fig. 6A). With regard to the in vitro culture after islet isolation, although islet viability in each group decreased gradually, that of the S-Kyoto group was well preserved compared with other isolation groups (Fig. 6B).

Improvement of Islet Function Elicited by Islet Isolation With S-Kyoto Solution

Next, we evaluated insulin function of islets using static glucose change. Although no significant difference was observed in insulin concentration under low glucose (2.8 mM) using each solution, insulin concentration under high glucose (20 mM) and the SI improved significantly by S-Kyoto islet isolation in comparison with those of other isolation solutions (Table 2). Based on the results of UW isolation groups (UW, S-UW), no beneficial effects of sivelestat were elicited as determined by the SI.

Prolongation of Islet Graft Survival in S-Kyoto Group and in In Vivo Experiments

Transplantation of 500 allogeneic islets of the ET-Kyoto group was associated with graft survival of 7.4± 1.1 days (Fig. 7A, Table 3). A significant prolongation of islet graft survival was noted after transplantation of the S-Kyoto group, compared with islet grafts of the ET-Kyoto group (11.2±1.3 days, p<0.05). Importantly, islet transplantation coupled with 15-day intraperitoneal administration of 2 mg/day sivelestat elicited significant prolongation of graft survival, compared with both ET-Kyoto and S-Kyoto groups, respectively (Fig. 7A, Table 3). Next, NE activity in sera of recipient mice was measured. NE activity increased gradually after islet transplantation in the S-Kyoto group. However, sivelestat significantly suppressed the enzyme activity measured at day 28 after transplantation (Fig. 7B). These results suggest that prolongation of islet graft survival in the sivelestat IP group is due to inhibition of NE enzyme activity and the anti-inflammatory properties of sivelestat.

To examine islet graft function in vivo, IPGTT was performed at day 7 after transplantation. In nondiabetic

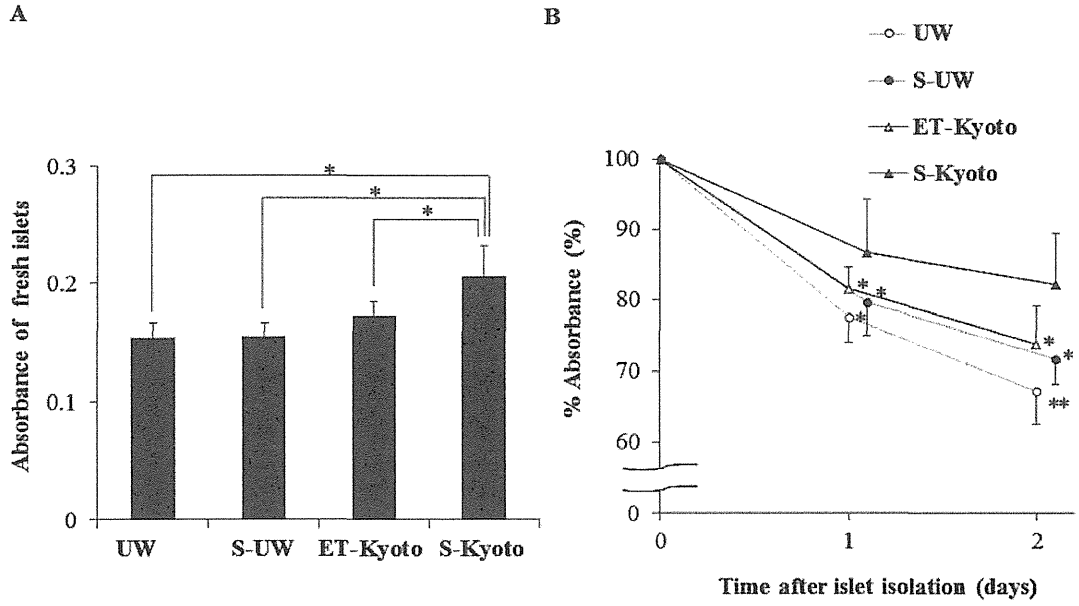

Figure 6. In vitro viability assay of isolated islets by MTS. (A) Viability of fresh islets (30 islets) was assessed using MTS assay. Data are mean ± SD of five independent experiments; $*p<0.05$. (B) Isolated islets (30 islets) were cultured for 0, 1, 2 days, and their viabilities were assessed by MTS assay. Data are mean ± SD of five independent experiments; $*p<0.05$, $**p<0.01$ versus fresh islets.

wild-type mice, injection of glucose-induced hyperglycemia with the peak blood glucose level recorded at 15 min, but the level returned to normal at 60–120 min after the injection (Fig. 7C). A similar pattern was observed in mice transplanted with S-Kyoto and S-Kyoto and treated with sivelestat. On the other hand, blood glucose levels of mice transplanted with ET-Kyoto group and untreated diabetic mice were significantly higher than those of the control wild-type mice before injection and at 15, 60, and 120 min after injection of glucose (Fig. 7C). Immunohistochemical staining for insulin confirmed that islet transplantation with S-Kyoto and S-Kyoto with sivelestat prolonged graft survival. Small islet grafts with many infiltrating inflammatory cells were detected at day 7 after transplantation in the ET-Kyoto group, whereas insulin-positive islet grafts with well preserved islet structure were found in the S-Kyoto and S-Kyoto with sivelestat groups (Fig. 7D).

Sivelestat Suppresses Proinflammatory Cytokines After Warm Digestion During Islet Isolation

We measured the levels of proinflammatory cytokines (IL-2, IL-4, IL-6, IL-10, IL-17A, IFN-γ, TNF-α) in the isolation solution at each step of islet isolation, including before warm digestion, at the end of warm digestion, and after purification. The levels at the end of warm digestion were markedly higher than before warm digestion (Fig. 8). On the other hand, IL-6 and TNF-α levels were significantly lower at the end of warm digestion in S-Kyoto solution compared with other isolation solutions such as UW and ET-Kyoto (Fig. 8).

Sivelestat Suppresses Proinflammatory Cytokines in Serum of Islet Recipients After Transplantation

The serum levels of IL-6 and TNF-α in islet recipients were significantly higher at 7 and 14 posttransplantation days than before transplantation (day −1), whereas no

Table 2. Insulin Concentration Under Low (2.8 mM) and High (20 mM) Glucose and Stimulation Index According to the Isolation Solution Used in the Present Study

	UW	S-UW	ET-Kyoto	S-Kyoto
Insulin concentration (μg/L) under:				
Low glucose (2.8 mM)	2.89 ± 0.37	2.75 ± 0.44	2.90 ± 0.30	2.98 ± 0.37
High glucose (20 mM)	3.68 ± 0.52¶	3.64 ± 0.54¶	3.78 ± 0.44¶	4.46 ± 0.79
Stimulation index (SI)	1.30 ± 0.06§	1.31 ± 0.12§	1.38 ± 0.12*	1.49 ± 0.08

Data are expressed as mean ± SD of five independent experiments. $*p<0.05$, ¶$p<0.01$, §$p<0.001$, compared with the S-Kyoto solution. SI was calculated as the ratio of insulin released during exposure to high glucose over the insulin released during low glucose incubation. SI, stimulation index; UW, University of Wisconsin.

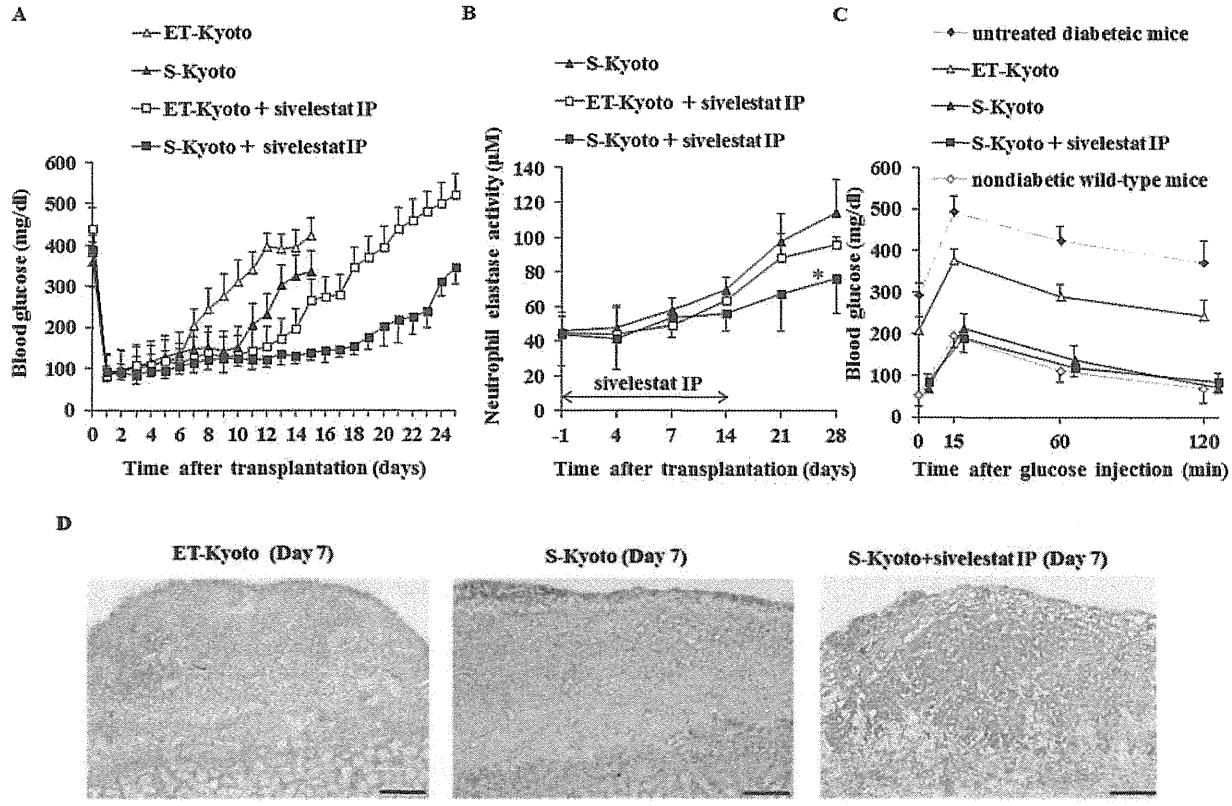

Figure 7. Results of in vivo transplant experiments. Islets were isolated using one of the isolation solutions (ET-Kyoto, S-Kyoto), then immediately transplanted (500 allogeneic islets) under the kidney capsule of diabetic mice. Sivelestat was injected intraperitoneally at 2 mg/day at 1 day before transplantation and every day until posttransplantation day 14. (A) Blood glucose levels of recipient mice transplanted with the islets. Data are mean ± SD of five independent mice. (B) Serum neutrophil elastase activity of recipient mice was measured at day 1 before transplantation and days 4, 7, 14, 21, 28 posttransplantation. Data are mean ± SD of three independent samples; $*p<0.05$, versus S-Kyoto. (C) IPGTT of recipient mice was performed at posttransplantation day 7. Blood glucose was measured in each group (nondiabetic wild-type mice, untreated diabetic mice, recipient mice transplanted with islets isolated by the use of ET-Kyoto, S-Kyoto, and S-Kyoto with sivelestat) before injection and at 15, 60, 120 min after injection. Data are mean ± SD of three independent mice. (D) Immunohistochemical analysis of insulin in a representative mouse kidney engrafted with islets was performed at posttransplantation day 7. Scale bars: 100 μm.

Table 3. Survival of Islet Allografts in Mice With Streptozotocin-Induced Diabetes

	Without Intraperitoneal Injection of Sivelestat		With Intraperitoneal Injection of Sivelestat	
	ET-Kyoto	S-Kyoto	ET-Kyoto	S-Kyoto
Graft survival (days)	6, 7, 8, 9	10, 11, 12, 13	12, 13, 14, 17, 20	18, 19, 20, 22, 26
Mean survival (days)	7.4 ± 1.1	11.2 ± 1.1¶	15.2 ± 3.3§	21.0 ± 3.2†

Data are mean ± SD of five independent experiments. ¶$p<0.01$, §$p<0.001$, compared with the ET-Kyoto isolation solution without intraperitoneal injection of sivelestat. †$p<0.001$, compared with the S-Kyoto isolation solution without intraperitoneal injection of sivelestat.

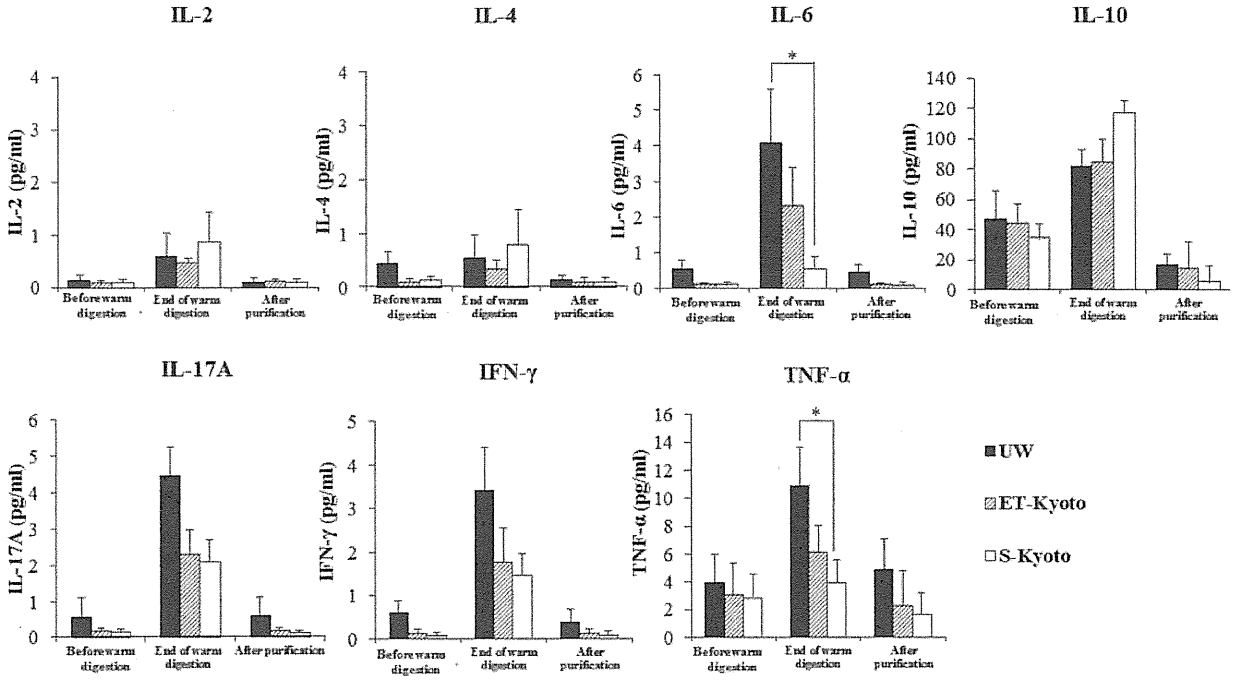

Figure 8. Assessment of proinflammatory cytokines in isolation solution during islet isolation. The levels of proinflammatory cytokines [interleukin (IL)-2, IL-4, IL-6, IL-10, IL-17A, interferon (IFN)-γ, tumor necrosis factor (TNF)-α] in the isolation solution were measured during islet isolation (before warm digestion, at the end of warm digestion, after purification). Data are mean±SD of four independent experiments; *$p<0.05$.

significant increases were noted in the levels of other cytokines except IL-6 and TNF-α (Fig. 9). The serum levels of IL-6 and TNF-α were significantly lower in the sivelestat intraperitoneal (IP) group compared with nonsivelestat IP group at 7 and 14 posttransplantation days (Fig. 9).

DISCUSSION

Islet transplantation is currently one of the most attractive strategies for the treatment of type 1 diabetes. One important key to achieving successful insulin independence after islet transplantation is acquiring a sufficient donor islet mass (1,10). The number and quality of islets recovered from isolation are influenced by several factors (10). Tissue damage of donor pancreas starts to occur as early as the onset of brain death associated with hypotension, peripheral vasoconstriction, tissue ischemia, and release of stress hormones and inflammatory mediators (10,20,24,38). Moreover, at the time of procurement, donor pancreas is exposed to warm ischemia after donor cross-clamping and cold ischemia storage in preservation solution, such as UW, ET-Kyoto solution (23,40). Furthermore, during islet isolation, warm digestion, trauma, and hypoxia may cause cell damage in isolated islets similar to ischemia/reperfusion injury (IRI) of other transplant organs (10). Therefore, we need to design an efficient isolation method to reduce cell damage toward donor pancreata.

The major finding of the present study was identification of the crucial role of NE in islet isolation and transplantation. First, we showed a marked increase in NE activity during islet isolation, especially at the end of warm digestion by collagenase (Fig. 2C), and that NE was cytotoxic against isolated islets (Fig. 1A). Second, the addition of sivelestat to the isolation solution during islet isolation inhibited NE activity (Fig. 2C) and significantly improved islet yields, islet viability, and insulin function of isolated islets (Tables 1 and 2). Furthermore, we also showed that treatment of recipient animals with sivelestat significantly prolonged the survival of insulin-secreting islet allografts (Fig. 7A, Table 3).

In clinical liver transplantation, IRI, an exogenous antigen-independent inflammatory event, remains a major problem, because IRI causes early transplant graft failure and can lead to a higher incidence of both acute and chronic rejections (6,54,55). The mechanisms underlying liver IRI involve leukocyte accumulation and activation of neutrophils, Kupffer cells (macrophages), and T cells, secretion of proinflammatory cytokines and chemokines, complement activation, and activation of vascular cell adhesion molecules (49,51,53–55). Recent reports also indicated that the cross-talk interaction between NE and

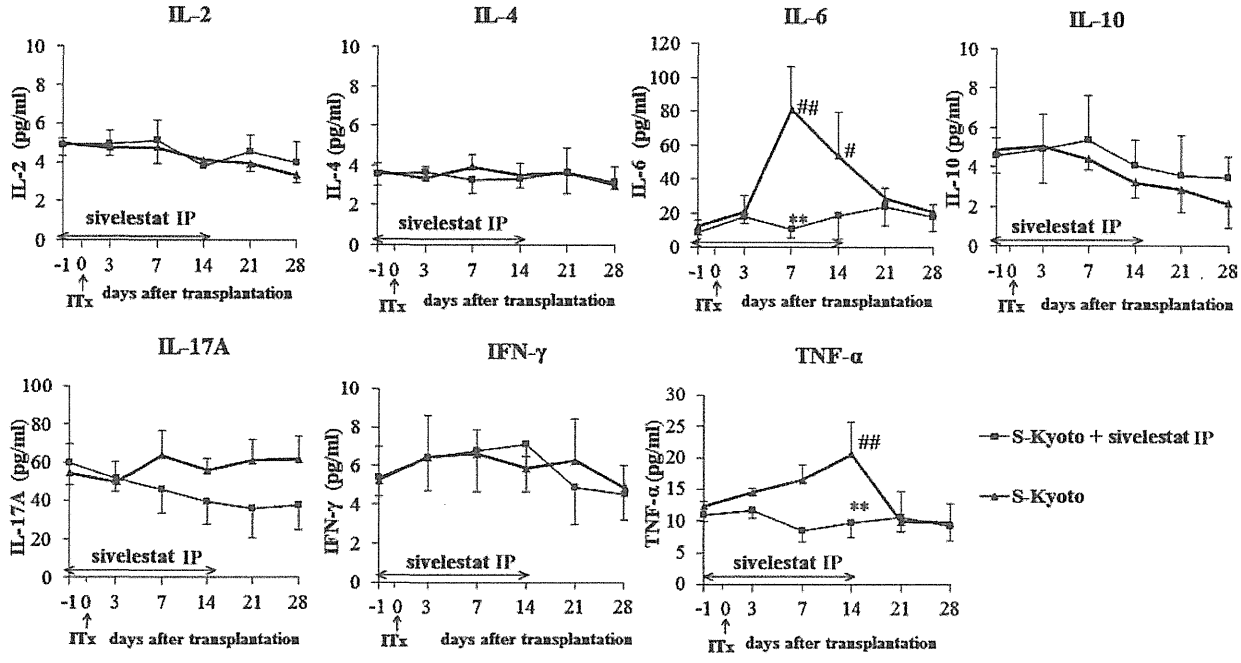

Figure 9. Assessment of proinflammatory cytokines in sera of islet mouse recipients after islet transplantation (ITx). The levels of proinflammatory cytokines (IL-2, IL-4, IL-6, IL-10, IL-17A, IFN-γ, TNF-α) in the sera of islet recipients were measured at pretransplantation day 1 and posttransplantation days 4, 7, 14, 21, and 28. Data are mean ± SD of three independent samples; $^{**}p<0.01$, versus nonsivelestat IP group, $\#p<0.05$ and $\#\#p<0.01$, versus before transplantation (day −1).

toll-like receptor (TLR) 4 promotes liver damage and that NE inhibitors, such as sivelestat, ameliorated the hepatocellular damage by reducing the expression of proinflammatory cytokines, chemokines, and TLR4 (24,54,55).

In islet transplantation, proinflammatory cytokines such as TNF-α and IL-1β induce β-cell apoptosis (1,3,27). These proinflammatory cytokines are produced by acinar and ductal cells (10). Moreover, in isolated islets, resident macrophages and monocytes produce cytokines (3,10,25). During islet isolation, the pancreatic tissues are warmed up to 37°C for collagenase digestion (10). As shown in Figure 2, many neutrophils were activated and released NE at the end of warm digestion. The released NE caused injury to membrane components of macrophages, acinar cells, and islets. Activated macrophages and acinar cells produce proinflammatory cytokines, including TNF-α and IL-6 (3). In fact, significantly high levels of TNF-α and IL-6 were found in isolation solution at the end of warm digestion compared with those before warm digestion (Fig. 8). Moreover, NE may also serve as a putative endogenous TLR4 ligand, causing TLR4 upregulation on macrophages and islets during the isolation process (5,39,54,55). Such excessive expression of TNF-α and TLR 4 affects the surrounding islets causing their apoptosis (7,19). Indeed, to detect apoptotic cells during islet isolation, TUNEL staining was performed before and at the end of warm digestion. Many TUNEL-positive cells were detected in UW solution at the end of warm digestion, whereas no such cells were detected in pancreatic tissue before warm digestion (Fig. 3A). What is the mechanism of NE-induced islet injury? Sivelestat effectively prevented the cross-talk between NE and inflammation responses, including the expression of proinflammatory cytokines (TNF-α, IL-6) and TLR4, resulting in a significant improvement in islet yields, islet viability, and insulin function in islet isolation with S-Kyoto solution. Furthermore, analysis of serum cytokine production profile (IL-2, IL-4, IL-6, IL-10, IL-17A, IFN-γ, TNF-α) in islet recipient mice showed significant increase in IL-6 and TNF-α production in serum at 1 and 2 weeks after islet transplantation, compared with those before islet transplantation (day −1), whereas no such increase was observed in the production of other cytokines before/after islet transplantation (Fig. 9). As shown in Figure 7B, NE activity increased gradually after islet transplantation. However, sivelestat significantly suppressed NE activity and the increase in IL-6 and TNF-α production in mice (Figs. 7B and 9). Taken together, local inflammatory reaction, resulting in functional loss of islet grafts occurred after transplantation and treatment with sivelestat inhibited such inflammatory reactions, as evidenced by reduced IL-6 and TNF-α production, and resulted in prolongation of islet allograft survival.

Trypsin released from pancreatic acinar cells directly destroys islets (35). Previous studies demonstrated that

inhibition of trypsin by pefabloc or ulinastatin during pancreas digestion improved islet yield and reduced the fraction of embedded islets (22,35). These findings suggest that trypsin may degrade pancreatic ductules, resulting in reduced delivery of collagenase solution (35). However, the molecular weight of the new recombinant NE inhibitor sivelestat is much lower than α1 protease inhibitors and appears to exert its cytoprotective effect in the microenvironment between neutrophil and pancreatic tissues (12,30). In this study, we examined the effects of the addition of sivelestat to ET-Kyoto solution. ET-Kyoto solution has a high-sodium/low-potassium composition with comparatively low viscosity (35). Therefore, it allows sufficient organ flushing after harvesting the pancreatic tissues (28,35). Furthermore, we also examined the effects of the addition of sivelestat to the UW solution. The results suggested that sivelestat also provided cytoprotection when added to the UW solution. This conclusion was based on the finding that the decrease in the number of activated neutrophils and neutrophil elastase activity in the S-UW group tended to be larger than in the UW group (Fig. 2B, C), albeit statistically insignificant. The islets isolated from the UW solution are easily damaged by mechanical stress due to the high viscosity of the UW solution (13). Indeed, in our experiment, membrane shear damage had a negative impact on the isolated islets of the UW group during the isolation process, as shown in Figure 4B. This was probably due to one or more of the following reasons: (1) higher viscosity of the UW solution relative to that of the ET-Kyoto solution, (2) the high percentage of activated neutrophils present in the pancreatic tissue, and (3) the higher level of neutrophil elastase released in the UW than in ET-Kyoto. We speculate that the balance between the amount of released neutrophil elastase and its inhibition by collagenase digestion tilts towards excess elastase activity when sivelestat is added to the UW solution. We also assessed the synergistic effects of ulinastatin and sivelestat on improvement of islet yield and islet viability. However, no additive effects were observed in comparison with S-Kyoto solution alone and S-Kyoto solution with ulinastatin (data not shown).

As shown in Figure 4B, SEM showed well-preserved islets that were isolated by S-Kyoto solution, as evident by their round and smooth surface. NE is reported to increase the permeability of vascular endothelial cells, a process known to be involved in tissue edema (30). Indeed, during islet isolation, inhibition of NE activity by sivelestat may maintain cell membrane stability and permeability of endothelial cells in isolated islets, preventing tissue edema and leading to improvement of islet yield and insulin function of isolated islets.

In conclusion, we succeeded in isolating large numbers of islets using a new preservation solution, S-Kyoto solution, and in significant prolongation of islet graft survival in recipient mice treated with sivelestat. Our results emphasize the role of NE in the pathophysiology of islet damage during islet isolation and after transplantation. NE contributes to the accumulation of neutrophils and secretion of proinflammatory mediators during the isolation procedure and after islet transplantation. Therefore, treatment with NE inhibitors is potentially suitable for better harvest of transplantable islets and long-term islet allograft survival, allowing successful management of diabetes with islets from a single donor. We plan to assess in the near future the beneficial effects of S-Kyoto solution and monotherapy with sivelestat in human islet transplantation.

ACKNOWLEDGMENTS: The authors thank Dr. F. G. Issa (www.word-medex.com.au) for the careful reading and editing of this manuscript, ONO Pharmaceutical Co. for kindly providing sivelestat, and Otsuka Pharmaceutical Co. for generously providing ET-Kyoto solution. The authors declare no conflict of interest.

REFERENCES

1. Abdelli, S.; Ansite, J.; Roduit, R.; Borsello, T.; Matsumoto, I.; Sawada, T.; Allaman-Pillet, N.; Henry, H.; Beckmann, J. S.; Hering B. J.; Bonny, C. Intracellular stress signaling pathways activated during human islet preparation and following acute cytokine exposure. Diabetes 53:2815–2823; 2004.
2. Andrikopoulos, S.; Blair, A. R.; Deluca, N.; Fam, B. C.; Proietto, J. Evaluating the glucose tolerance test in mice. Am. J. Physiol. Endocrinol. Metab. 295:E1323–E1332; 2008.
3. Barshes, N. R.; Wyllie, S.; Goss, J. A. Inflammation-mediated dysfunction and apoptosis in pancreatic islet transplantation: Implications for intrahepatic grafts. J. Leukoc. Biol. 77:587–597; 2005.
4. Bottino, R.; Balamurugan, A. N.; Tse, H.; Thirunavukkarasu, C.; Ge, X.; Profozich, J.; Milton, M.; Ziegenfuss, A.; Trucco, M.; Piganelli, J. D. Response of human islets to isolation stress and the effect of antioxidant treatment. Diabetes 53:2559–2568; 2004.
5. Devaney, J. M.; Greene, C. M.; Taggart, C. C.; Carroll, T. P.; O'Neill, S. J.; McElvaney, N. G.; Neutrophil elastase upregulates interleukin-8 via toll-like receptor 4. FEBS Lett. 544:129–132; 2003.
6. Farmer, D. G.; Amersi, F.; Kupiec-Weglinski, J.; Busuttil, R. W. Current status of ischemia and reperfusion injury in the liver. Transplant. Rev. 14:106–126; 2000.
7. Gao, Q.; Ma, L. L.; Gao, X.; Yan, W.; Williams, P.; Yin, D. P. TLR 4 mediates early graft failure after intraportal islet transplantation. Am. J. Transplant. 10:1588–1596; 2010.
8. Hering, B. J. Achieving and maintaining insulin independence in human islet transplant recipients. Transplantation 79:1296–1297; 2005.
9. Ichii, H.; Pileggi, A.; Molano, R. D.; Baidal, D. A.; Khan, A.; Kuroda, Y.; Inverardi, L.; Goss, J. A.; Alejandro, R.; Ricordi, C. Rescue purification maximizes the use of human islet preparations for transplantation. Am. J. Transplant. 5:21–30; 2005.

10. Ito, T.; Omori, K.; Rawson, J.; Todorov, I.; Asari, S.; Kuroda, A.; Shintaku, J.; Itakura, S.; Ferreri, K.; Kandeel, F.; Mullen, Y. Improvement of canine islet yield by donor pancreas infusion with a p38 MAPK inhibitor. Transplantation. 86:321–329; 2008.
11. Kawabata, K.; Hagio, T.; Matsumoto, S.; Nakao, S.; Orita, S.; Aze, Y.; Ohno, H. Delayed neutrophil elastase inhibition prevents subsequent progression of acute lung injury induced by endotoxin inhalation in hamsters. Am. J. Respir. Crit. Care Med. 161:2013–2018; 2000.
12. Kawabata, K.; Suzuki, M.; Sugitani, M.; Imaki, K.; Toda, M.; Miyamoto, T. ONO-5046, a novel inhibitor of human neutrophil elastase. Biochem. Biophys. Res. Commun. 17: 814–820; 1991.
13. Kenmochi, T.; Miyamoto, M.; Sasaki, H.; Une, S.; Nakagawa, Y.; Moldovan, S.; Benhamou, P. Y.; Brunicardi, F. C.; Tanaka, H.; Mullen, Y. LAP-1 cold preservation solution for isolation of high-quality human pancreatic islets. Pancreas 17:367–377; 1998.
14. Khandoga, A.; Huettinger, S.; Khandoga, A. G.; Li, H.; Butz, S.; Jauch, K. W.; Vestweber, D.; Krombach, F. Leukocyte transmigration in inflamed liver: A role for endothelial cell-selective adhesion molecule. J. Hepatol. 50:755–765; 2009.
15. Kin, T.; Johnson, P. R.; Shapiro, A. M.; Lakey, J. R. Factors influencing the collagenase digestion phase of human islet isolation. Transplantation 83:7–12; 2007.
16. Kin, T.; Zhai, X.; Murdoch, T. B.; Salam, A.; Shapiro, A. M.; Lakey, J. R. Enhancing the success of human islet isolation through optimization and characterization of pancreas dissociation enzyme. Am. J. Transplant. 7:1233–1241; 2007.
17. Kono, T.; Okada, S.; Saito, M. Neutrophil elastase inhibitor, sivelestat sodium hydrate prevents ischemia-reperfusion injury in the rat bladder. Mol. Cell. Biochem. 311:87–92; 2008.
18. Korsgren, O.; Lundgren, T.; Felldin, M.; Foss, A.; Isaksson, B.; Permert, J.; Persson, N. H.; Rafael, E.; Rydén, M.; Salmela, K.; Tibell, A.; Tufveson, G.; Nilsson, B. Optimising islet engraftment is critical for successful clinical islet transplantation. Diabetologia 51:227–232; 2008.
19. Krüger, B.; Yin, N.; Zhang, N.; Yadav, A.; Coward, W.; Lal, G.; Zang, W.; Heeger, P. S.; Bromberg, J. S.; Murphy, B.; Schröppel, B. Islet-expressed TLR 2 and TLR 4 sense injury and mediate early graft failure after transplantation. Eur. J. Immunol. 40:2914–2924; 2010.
20. Kusaka, M.; Pratschke, J.; Wilhelm, M. J.; Ziai, F.; Zandi-Nejad, K.; Mackenzie, H. S.; Hancock, W. W.; Tilney, N. L. Activation of inflammatory mediators in rat renal isografts by donor brain death. Transplantation 69:405–410; 2000.
21. Kwon, A. H.; Qiu, Z. Neutrophil elastase inhibitor prevents endotoxin-induced liver injury following experimental partial hepatectomy. Br. J. Surg. 94:609–619; 2007.
22. Lakey, J. R.; Helm, L. M.; Kin, T.; Korbutt, G. S.; Rajotte, R. V.; Shapiro, A. M.; Warnock, G. L. Serine-protease inhibition during islet isolation increases islet yield from human pancreases with prolonged ischemia. Transplantation 72: 565–570; 2001.
23. Lakey, J. R.; Rajotte, R. V.; Warnock, G. L.; Kneteman, N. M. Human pancreas preservation prior to islet isolation. Cold ischemic tolerance. Transplantation 59:689–694; 1995.
24. Land, W. G. The role of postischemic reperfusion injury and other nonantigen-dependent inflammatory pathways in transplantation. Transplantation 79:505–514; 2005.
25. Lawrence, M. C.; Naziruddin, B.; Levy, M. F.; Jackson, A.; McGlynn, K. Calcineurin/nuclear factor of activated T cells and MAPK signaling induce TNF-{alpha} gene expression in pancreatic islet endocrine cells. J. Biol. Chem. 286:1025–1036; 2011.
26. Li, D. S.; Yuan, Y. H.; Tu, H. J.; Liang, Q. L.; Dai, L. J. A protocol for islet isolation from mouse pancreas. Nat. Protoc. 4:1649–1652; 2009.
27. Linn, T.; Schmitz, J.; Hauck-Schmalenberger, I.; Lai, Y.; Bretzel, R. G.; Brandhorst, H.; Brandhorst, D. Ischemia is linked to inflammation and induction of angiogenesis in pancreatic islets. Clin. Exp. Immunol. 144:179–187; 2006.
28. Matsumoto, S.; Noguchi, H.; Shimoda, M.; Ikemoto, T.; Naziruddin, B.; Jackson, A.; Tamura, Y.; Olson, G.; Fujita, Y.; Chujo, D.; Takita, M.; Kobayashi, N.; Onaca, N.; Levy, M. Seven consecutive successful clinical islet isolations with pancreatic ductal injection. Cell Transplant. 19:291–297; 2010.
29. Moberg, L.; Korsgren, O.; Nilsson, B. Neutrophil granulocytes are the predominant cell type infiltrating pancreatic islets in contact with ABO-compatible blood. Clin. Exp. Immunol. 142:125–131; 2005.
30. Mori, H.; Nagahiro, I.; Osaragi, T.; Kotani, K.; Nakanishi, H.; Sano, Y.; Date, H.; Shimizu, N. Addition of a neutrophil elastase inhibitor to the organ flushing solution decreases lung reperfusion injury in rat lung transplantation. Eur. J. Cardiothorac. Surg. 32:791–795; 2007.
31. Morini, S.; Braun, M.; Onori, P.; Cicalese, L.; Elias, G.; Gaudio, E.; Rastellini, C. Morphological changes of isolated rat pancreatic islets: A structural, ultrastructural and morphometric study. J. Anat. 209:381–392; 2006.
32. Morohoshi, Y.; Matsuoka, K.; Chinen, H.; Kamada, N.; Sato, T.; Hisamatsu, T.; Okamoto, S.; Inoue, N.; Takaishi, H.; Ogata, H.; Iwao, Y.; Hibi, T. Inhibition of neutrophil elastase prevents the development of murine dextran sulfate sodium-induced colitis. J. Gastroenterol. 41:318–324; 2006.
33. Noguchi, H.; Nakai, Y.; Matsumoto, S.; Kawaguchi, M.; Ueda, M.; Okitsu, T.; Iwanaga, Y.; Yonekawa, Y.; Nagata, H.; Minami, K.; Masui, Y.; Futaki, S.; Tanaka, K. Cell Permeable peptide of JNK inhibitor prevents islet apoptosis immediately after isolation and improves islet graft function. Am. J. Transplant. 5:1848–1855; 2005.
34. Noguchi, H.; Naziruddin, B.; Onaca, N.; Jackson, A.; Shimoda, M.; Ikemoto, T.; Fujita, Y.; Kobayashi, N.; Levy, M. F.; Matsumoto, S. Comparison of modified Celsior solution and M-Kyoto solution for pancreas preservation in human islet isolation. Cell Transplant. 19:751–758; 2010.
35. Noguchi, H.; Ueda, M.; Nakai, Y.; Iwanaga, Y.; Okitsu, T.; Nagata, H.; Yonekawa, Y.; Kobayashi, N.; Nakamura, T.; Wada, H.; Matsumoto, S. Modified two–zlayer preservation method (M-Kyoto/PFC) improves islet yields in islet isolation. Am. J. Transplant. 6:496–504; 2006.
36. Ohmura, Y.; Tanemura, M.; Kawaguchi, N.; Machida, T.; Tanida, T.; Deguchi, T.; Wada, H.; Kobayashi, S.; Marubashi, S.; Eguchi, H.; Takeda, Y.; Matsuura, N.; Ito, T.; Nagano, H.; Doki, Y.; Mori, M. Combined transplantation of pancreatic islets and adipose tissue-derived stem cells enhances the survival and insulin function of islet grafts in diabetic mice. Transplantation 90:1366–1373; 2010.
37. Paraskevas, S.; Maysinger, D.; Wang, R.; Duguid, T. P.; Rosenberg, L. Cell loss in isolated human islets occurs by apoptosis. Pancreas 20:270–276; 2000.

38. Pratschke, J.; Wilhelm, M. J.; Kusaka, M.; Basker, M.; Cooper, D. K.; Hancock, W. W.; Tilney, N. L. Brain death and its influence on donor organ quality and outcome after transplantation. Transplantation 67:343–348; 1999.
39. Ribeiro-Gomes, F. L.; Moniz-de-Souza, M. C.; Alexandre-Moreira, M. S.; Dias, W. B.; Lopes, M. F.; Nunes, M. P.; Lungarella, G.; Dos Reis, G. A. Neutrophils activate macrophages for intracellular killing of *Leishmania major* through recruitment of TLR 4 by neutrophil elastase. J. Immunol. 179:3988–3994; 2007.
40. Ricordi, C. Quantitative and qualitative standards for islet isolation assessment in humans and large mammals. Pancreas 6:242–244; 1991.
41. Ricordi, C.; Strom, T. B. Clinical islet transplantation: Advances and immunological challenges. Nat. Rev. Immunol. 4:259–268; 2004.
42. Rosenberg, L.; Wang, R.; Paraskevas, S.; Maysinger, D. Structural and functional changes resulting from islet isolation lead to islet cell death. Surgery 126:393–398; 1999.
43. Ryan, E. A.; Lakey, J. R.; Paty, B. W.; Imes, S.; Korbutt, G. S.; Kneteman, N. M.; Bigam, D.; Rajotte, R. V.; Shapiro, A. M. Successful islet transplantation: Continued insulin reserve provides long-term glycemic control. Diabetes 51:2148–2157; 2002.
44. Ryan, E. A.; Lakey, J. R.; Rajotte, R. V.; Korbutt, G. S.; Kin, T.; Imes, S.; Rabinovitch, A.; Elliott, J. F.; Bigam, D.; Kneteman, N. M.; Warnock, G. L.; Larsen, I.; Shapiro, A. M. Clinical outcomes and insulin secretion after islet transplantation with the Edmonton protocol. Diabetes 50:710–719; 2001.
45. Ryan, E. A.; Paty, B. W.; Senior, P. A.; Bigam, D.; Alfadhli, E.; Kneteman, N. M.; Lakey, J. R.; Shapiro, A. M. Five-year follow-up after clinical islet transplantation. Diabetes 54:2060–2069; 2005.
46. Shapiro, A. M.; Lakey, J. R.; Paty, B. W.; Senior, P. A.; Bigam, D. L.; Ryan, E. A. Strategic opportunities in clinical islet transplantation. Transplantation 79:1304–1307; 2005.
47. Shapiro, A. M.; Lakey, J. R.; Ryan, E. A.; Korbutt, G. S.; Toth, E.; Warnock, G. L.; Kneteman, N. M.; Rajotte, R. V. Islet transplantation in seven patients with type 1 diabetes mellitus using a glucocorticoid-free immunosuppressive regimen. N. Engl. J. Med. 343:230–238; 2000.
48. Shapiro, A. M.; Ricordi, C.; Hering, B. J.; Auchincloss, H.; Lindblad, R.; Robertson, R. P.; Secchi, A.; Brendel, M. D.; Berney, T.; Brennan, D. C.; Cagliero, E.; Alejandro, R.; Ryan, E. A.; DiMercurio, B.; Morel, P.; Polonsky, K. S.; Reems, J. A.; Bretzel, R. G.; Bertuzzi, F.; Froud, T.; Kandaswamy, R.; Sutherland, D. E.; Eisenbarth, G.; Segal, M.; Preiksaitis, J.; Korbutt, G. S.; Barton, F. B.; Viviano, L.; Seyfert-Margolis, V.; Bluestone, J.; Lakey, J. R. International trial of the Edomonton protocol for islet transplantation. N. Engl. J. Med. 355:1318–1330; 2006.
49. Shimoda, M.; Iwasaki, Y.; Okada, T.; Sawada, T.; Kubota, K. Protective effect of sivelestat in a porcine hepatectomy model prepared using an intermittent Pringle method. Eur. J. Pharmacol. 587:248–252; 2008.
50. Tamakuma, S.; Ogawa, M.; Aikawa, N.; Kubota, T.; Hirasawa, H.; Ishizaka, A.; Tanaka, N.; Hamada, C.; Matsuoka, S.; Abiru, T. Relationship between neutrophil elastase and acute lung injury in humans. Pulm. Pharmacol. Ther. 17:271–279; 2004.
51. Teoh, N. C.; Farrell, G. C. Hepatic ischemia reperfusion injury: Pathogenic mechanisms and basis for hepatoprotection. J. Gastroenterol. Hepatol. 18:891–902; 2003.
52. Thomas, F.; Wu, J.; Contreras, J. L.; Smyth, C.; Bilbao, G.; He, J.; Thomas, J. A tripartite anoikis-like mechanism causes early isolated islet apoptosis. Surgery 130:333–338; 2001.
53. Tsuchihashi, S.; Ke, B.; Kaldas, F.; Flynn, E.; Busuttil, R. W.; Briscoe, D. M.; Kupiec-Weglinski, J. W. Vascular endothelial growth factor antagonist modulates leukocyte trafficking and protects mouse livers against ischemia/reperfusion injury. Am. J. Pathol. 168:695–705; 2006.
54. Uchida, Y.; Freitas, M. C.; Zhao, D.; Busuttil, R. W.; Kupiec-Weglinski, J. W. The inhibition of neutrophil elastase ameliorates mouse liver damage due to ischemia and reperfusion. Liver Transpl. 15:939–947; 2009.
55. Uchida, Y.; Freitas, M. C.; Zhao, D.; Busuttil, R. W.; Kupiec-Weglinski, J. W. The protective function of neutrophil elastase inhibitor in liver Ischemia/reperfusion injury. Transplantation 89:1050–1056; 2010.
56. Wang, P.; Henning, S. M.; Heber, D. Limitations of MTT and MTS-based assays for measurement of antiproliferative activity of green tea polyphenols. PLoS One 5:e10202; 2010.
57. Wu, Y.; Han, B.; Luo, H.; Roduit, R.; Salcedo, T. W.; Moore, P. A.; Zhang, J.; Wu, J. DcR3/TR6 effectively prevents islet primary nonfunction after transplantation. Diabetes 52:2279–2286; 2003.
58. Yin, D.; Ding, J. W.; Shen, J.; Ma, L.; Hara, M.; Chong, A. S. Liver ischemia contributes to early islet failure following intraportal transplantation: Benefits of liver ischemic-preconditioning. Am. J. Transplant. 6:60–68; 2006.
59. Yoshimura, K.; Nakagawa, S.; Koyama, S.; Kobayashi, T.; Homma, T. Roles of neutrophil elastase and superoxide anion in leukotriene B4-induced lung injury in rabbit. J. Appl. Physiol. 76:91–96; 1994.
60. Zeiher, B. G.; Artigas, A.; Vincent, J. L.; Dmitrienko, A.; Jackson, K.; Thompson, B. T.; Bernard, G. Neutrophil elastase inhibition in acute lung injury: Results of the STRIVE study. Crit. Care Med. 32:1695–1702; 2004.

American Journal of Transplantation 2012; 12: 102–114
Wiley Periodicals Inc.

doi: 10.1111/j.1600-6143.2011.03771.x

Rapamycin Causes Upregulation of Autophagy and Impairs Islets Function Both *In Vitro* and *In Vivo*

M. Tanemura[a,*], Y. Ohmura[a], T. Deguchi[a], T. Machida[a], R. Tsukamoto[a], H. Wada[a], S. Kobayashi[a], S. Marubashi[a], H. Eguchi[a], T. Ito[b], H. Nagano[a], M. Mori[a] and Y. Doki[a]

Departments of [a]Gastroenterological Surgery and [b]Complementary and Alternative Medicine, Osaka University Graduate School of Medicine, Osaka, Japan
**Corresponding author: Masahiro Tanemura, mtanemura@gesurg.med.osaka-u.ac.jp*

Autophagy is a lysosomal degradation process of redundant or faulty cell components in normal cells. However, certain diseases are associated with dysfunctional autophagy. Rapamycin, a major immunosuppressant used in islet transplantation, is an inhibitor of mammalian target of rapamycin and is known to cause induction of autophagy. The objective of this study was to evaluate the *in vitro* and *in vivo* effects of rapamycin on pancreatic β cells. Rapamycin induced upregulation of autophagy in both cultured isolated islets and pancreatic β cells of green fluorescent protein–microtubule-associated protein 1 light chain 3 transgenic mice. Rapamycin reduced the viability of isolated β cells and down-regulated their insulin function, both *in vitro* and *in vivo*. In addition, rapamycin increased the percentages of apoptotic β cells and dead cells in both isolated and *in vivo* intact islets. Treatment with 3-methyladenine, an inhibitor of autophagy, abrogated the effects of rapamycin and restored β-cell function in both *in vitro* experiments and animal experiments. We conclude that rapamycin-induced islet dysfunction is mediated through upregulation of autophagy, with associated downregulation of insulin production and apoptosis of β cells. The results also showed that the use of an autophagy inhibitor abrogated these effects and promoted islet function and survival. The study findings suggest that targeting the autophagy pathway could be beneficial in promoting islet graft survival after transplantation.

Key words: Autophagy, islet transplantation, LC3, rapamycin, transgenic mice

Abbreviations: Atg gene, autophagy related gene; BSA, bovine serum albumin; FKBP-12, 12-kDa FK506-binding protein; GFP, green fluorescent protein; GAPDH, glyceraldehyde-3-phosphate; LC3, microtubule-associated protein 1 light chain 3; mTOR, mammalian target of rapamycin; PBS, phosphate-buffered saline; TUNEL, terminal deoxynucleotidyl transferase-mediated dUTP nick-end labeling; SD, standard deviation.

Received 18 March 2011, revised 22 August 2011 and accepted for publication 22 August 2011

Introduction

Autophagy, i.e. "self-eating", is an intracellular degradation system designed for degradation of cytoplasmic proteins and dysfunctional organelles after their sequestration in the autophagosome. To date, only microtubule-associated protein1 light chain 3 (LC3), a mammalian homolog of yeast autophagy related gene8 (Atg8), is known to exist in the autophagosomes, and therefore this protein serves as a marker for autophagosomes (1–3). The process is tightly regulated and plays an important role in cell growth, development and homeostasis, where it helps to maintain a balance between the synthesis, degradation and subsequent recycling of cellular components (1–3). Autophagy is induced dynamically by nutrient depletion to provide necessary amino acids within cells, thus helping them adapt to starvation (4). The physiological role of autophagy has been studied in various organisms and current knowledge indicates that autophagy is involved not only in adaptation to starvation but also in the quality control of intracellular proteins and organelles, to maintain cell functions, development, growth, clearance of intracellular microbes, antigen presentation and protection against disease (5–11). Thus, autophagy functions as a cell-protective mechanism and is up-regulated when cells are preparing to rid themselves of damaging cytoplasmic components, for example, during infection or protein aggregate accumulation (12).

Rapamycin is a macrolide fungicide with immunosuppressant properties that bear molecular structural similarities to the calcineurin inhibitor, tacrolimus (13). However, the mechanism of action of rapamycin is distinct from that of calcineurin inhibitor, such as cyclosporine and tacrolimus. Rapamycin binds to its intracellular receptor, the immunophilin 12-kDa FK506-binding protein (FKBP-12) and the rapamycin-FKBP-12 complex binds to and inhibits the mammalian target of rapamycin (mTOR; Ref. 14). Inhibition of mTOR leads to arrest of the cell cycle at the G1 to S phase and thus, blockade of growth-factor-driven proliferation of not only activated T cells, which constitute the basis of its immunosuppressive action, but also

other hematopoietic and nonhematopoietic cells (14,15). The mTOR is ubiquitously expressed in various cell types and functionally is a serine/threonine protein kinase that regulates important cellular process, including growth, proliferation, motility, survival, protein synthesis and transcription (16). Furthermore, activation of mTOR leads to inhibition of autophagy in cells ranging from yeast to human (17). Based on the above background, it is conceivable that the inhibitory action of rapamycin on mTOR activity induces autophagy in pancreatic islets.

Islet transplantation was recently advanced by the publication of the results of the Edmonton Protocol of immunosuppressive regimen, leading to insulin independence at 1 year in 90% of patients treated with type 1 diabetes (18–21). Accordingly, rapamycin has become a part of the standard treatment in islet transplantation. Its effectiveness in preventing allorejection and autoimmunity and promoting the survival of regulatory T lymphocytes has contributed to widespread use (22–24). However, recent reports described gradual deterioration of the metabolic profile and the need for reintroduction of exogenous insulin; only 10% of islet recipients maintained insulin independence at 5 years (21,25,26). Although the cause of the decline in insulin independence rates after islet transplantation remains obscure, the decline may reflect toxicity associated with long-term use of immunosuppressive drugs on islet β cells.

The effects of calcineurin inhibitors on islet function and proliferation have been recognized (27,28), although increasing data suggest that rapamycin alone or in combination with tacrolimus could impair islet cell function and survival (29–31). In addition, the antiangiogenic and antiproliferative properties of rapamycin could also prevent vascularization of transplanted islets, with a resultant reduction of posttransplantation engrafted and surviving islet mass (32–34).

Although it has been reported that β cells of ZDF rats (a rodent model of type 2 diabetes) contain a significant number of autophagic vacuoles (35), there is little information on the physiopathological roles of autophagy in the islets, and no causal link has been reported between autophagy and pathogenesis of diabetes. The aims of this study were to evaluate the *in vitro* and *in vivo* effects of rapamycin on pancreatic β cells, including induction of autophagy, cell viability and insulin secretory function, because these factors may contribute to progressive dysfunction of islet grafts in recipients.

Materials and Methods

In vitro *autophagy induction assay and islet viability assay*

Thirty cells from fresh mice islets, obtained from either C57BL/6 mice or green fluorescent protein (GFP)–LC3 transgenic mice were seeded in a 96-well culture plate and cultured for either 24 or 48 h with complete culture medium containing 1 or 10 ng/mL of rapamycin. In the first step, treated islets that were isolated from transgenic mice were observed by fluorescence microscopy to detect GFP signals, which is an accurate marker of induction of autophagy (36). Subsequently, islet viability was evaluated after 24 h treatment by monitoring metabolic activity with the colorimetric methyl tetrazolium salt (MTS) assay using the Cell Titer 96 Aqueous One reagent (Promega, Madison, WI, USA; Ref. 37). The colorimetric reagent was added to each well of the plate and incubated for 2 h, and the absorbance values read at 490 nm.

To further determine the change in islet viability before/after rapamycin treatment, fluorescence labeling was performed using tetramethyl rhodamine ethyl ester (TMRE; Molecular Probes, Eugene, OR, USA) and 7-amino actinomycin D (7-AAD; Molecular Probes; Refs. 38,39). Islets treated or untreated with rapamycin were dissociated into single cell suspensions, using Accutase (Innovative Cell Technologies Inc, San Diego, CA, USA). The dispersed cell suspensions were stained with Newport Green PDX acetoxymethylether (Molecular Probes), for identification of β cells (38). The single islet cell suspensions were incubated with 100 ng/mL TMRE for 30 min at 37°C in phosphate-buffered saline (PBS) without Ca^{2+} and Mg^{2+}. This dye selectively binds to the mitochondrial membrane allowing the assessment of cells with functional mitochondria, and therefore is a good marker for cell viability. Furthermore, cells were stained with 7-AAD that binds to DNA when cell membrane permeability is altered after cell death. Stained cells were analyzed by FACSCalibur flow cytometer (BD Immunocytometry, San Jose, CA, USA). In addition, improvement in islet viability was assessed by either MTS assay, TMRE or 7-AAD staining based on the results of autophagic signal blocking. Islet viability assays were performed with the addition of 10 mM of 3-methyladenine (3-MA).

Glucose-stimulated insulin release and stimulation index (SI)

To determine the changes in the endocrinological potency of rapamycin-treated islets, static glucose challenge was performed with or without 1 or 10 ng/mL of rapamycin. After overnight culture with or without rapamycin, 100 IEQ of treated islets were incubated with either 2.8 or 20 mM of glucose in culture medium for 2 h at 37°C to stimulate insulin release. The supernatants were collected and stored at −80°C for insulin assessment by enzyme-linked immunosorbent assay (ELISA; Mercodia Inc., Uppsala, Sweden; Refs. 38–40). Glucose-stimulated insulin release was expressed as the SI, calculated as the ratio of insulin released during exposure to high glucose (20 mM) over that released during low glucose incubation (2.8 mM). To determine the *in vitro* islet potency with regard to autophagic signal blocking, static incubation was also performed with the addition of 10 mM of 3-MA.

In vivo *studies using GFP-LC3 transgenic mice*

To study the effects of starvation, transgenic mice were provided with drinking water *ad libitum*, but were deprived of food for 24 h (10 a.m.–10 a.m.; Ref. 36). The starved transgenic mice were sacrificed and the pancreas, brain and muscle tissues were recovered. This was followed by preparation of the tissues for fluorescence microscopy. Furthermore, to demonstrate *in vivo* 3-MA-induced blocking of autophagy, mice were injected intraperitoneally (i.p.) with 10 mM of 3-MA for 2 weeks, followed by starvation for 24 h.

To assess the *in vivo* effects of rapamycin on islets from GFP-LC3 transgenic mice, mice were randomly separated into three experimental groups, no treatment group (i.e. control group; n = 25), rapamycin-treated group (n = 25) and the combination treatment group (n = 25) treated with both rapamycin and 3-MA. Rapamycin treatment consisted of daily i.p. injection of 0.2 mg/kg rapamycin and combined treatment consisted of daily i.p. injection of 0.2 mg/kg rapamycin combined with 10 mM of 3-MA. These treatments continued for 1, 2, 3, 4 or 5 weeks (n = 5 mice, each). The rapamycin-treated transgenic mice were sacrificed, the pancreas was removed and

processed for fluorescence and immunofluorescence microscopy. During rapamycin treatment, nonfasting blood glucose level was monitored daily using samples obtained from the tail vein. To further determine the effects of rapamycin on glucose tolerance, intraperitoneal glucose tolerance test (IPGTT) was conducted before and at days 14 and 28 after treatment (41). In this test, mice were fasted for 6 h and then injected intraperitoneally with 2 g glucose in saline/kg body weight. Blood glucose levels were measured for 2 h at 30 min intervals. Moreover, to detect the change in insulin secretion after *in vivo* rapamycin treatment, plasma insulin levels were also measured by ELISA before and after the treatment (at days 0, 7, 14, 21, 28 and 35, n = 5 mice, each group).

Fluorescence microscopy and immunofluorescence microscopy

Pancreatic tissue samples for GFP examination were prepared as follows. To prevent artificial induction of autophagy during sample preparation, mice were anesthetized by diethyl ether and immediately fixed by transcardial perfusion through the left ventricle with 4% paraformaldehyde dissolved in 0.1 M Na-phosphate buffer (pH 7.4). Subsequently, the pancreas was removed and further fixed with the same fixative for another 4 h at room temperature, followed by treatment with 5% sucrose in PBS for 2 h and then with 15% sucrose solution for 4 h, finally with 30% sucrose solution overnight. Pancreatic tissue samples were embedded in Tissue-Tek OCT compound (Sakura Finetechnical Co., Tokyo, Japan) and stored at −80°C. The tissue samples were sectioned at 7 μm thickness with a cryostat, air-dried for 30 min at room temperature and then stored at −80°C until use. Fluorescence signals were analyzed by Biozero fluorescence microscopy (Keyence, Osaka, Japan) by measuring green fluorescence (excitation, 488 nm; emission, 530 nm).

For general histological examination, cryosections were stained with hematoxylin and eosin. Furthermore, for immunofluorescence microscopy, cryosections were prepared as described earlier. After rinsing with water for 5 min, the sections were blocked with 4% bovine serum albumin (BSA)–PBS for 10 min at room temperature. Subsequently, these sections were incubated with rabbit polyclonal anti-mouse insulin Ab (SC-9168; Santa Cruz Biotechnology, Santa Cruz, CA, USA) overnight at 4°C diluted in 1% BSA-TBS-Tween-20 (0.05% w/v), followed by incubation with Alexa fluor555 goat anti-mouse IgG (H+L) Ab (A21429; 1:1000 dilution; Invitrogen, Carlsbad, CA, USA) for 30 min at room temperature. Fluorescence signals were observed by Biozero fluorescence microscopy (Keyence). The fluorescence intensities of insulin and GFP-LC3 in treated islets were quantified using Fluor-Chem image analyzer (Bio-Rad Laboratories Inc., Hercules, CA, USA) and expressed in arbitrary units. The mean fluorescence intensities of insulin and GFP, expressed as mean ± standard deviation (SD), were determined in islets of five rapamycin-treated mice. To identify apoptotic β cells in the pancreas of mice, islet sections were stained with terminal deoxynucleotidyl transferase-mediated dUTP nick-end labeling (TUNEL) using Tumor TACS™ *In Situ* Apoptosis Detection Kit (catalog# 4815–30-K, Trevigen, Gaithersburg, MD, USA) following the instructions provided by the manufacturer.

Statistical analysis

Data were expressed as mean ± SD and analyzed using Excel for Windows software. Two samples were compared with the Student's *t*-test. The p values <0.05 denoted the presence of statistical significance.

Details of the mice used in these experiments, islet isolation to assess the effects of rapamycin treatment *in vitro* and western blot analysis are presented in the Supplementary Materials and Methods in the on line version of the journal.

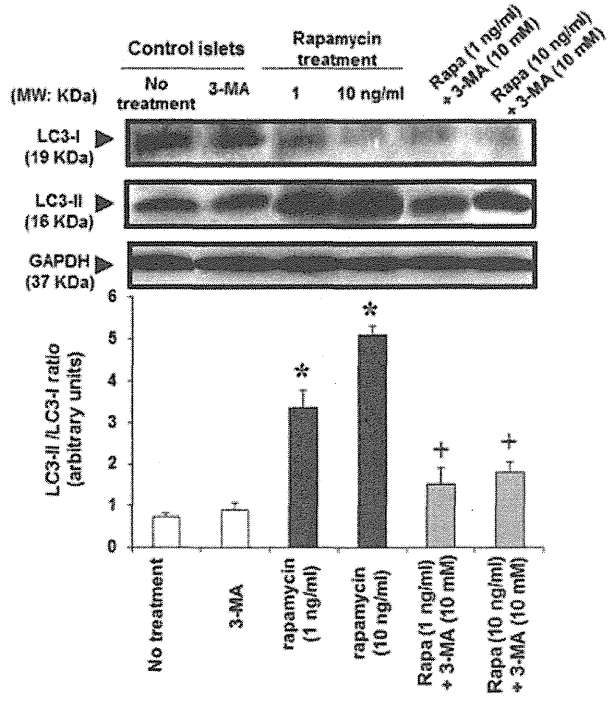

Figure 1: Changes in LC3-I and LC3-II protein expression levels in rapamycin-treated islets. LC3-I and LC3-II protein expression level were examined by western blot analysis. Protein samples extracted from either untreated islets, rapamycin-treated or rapamycin + 3-MA-treated islets were subjected to 15% SDS/PAGE and transferred onto PVDF membrane. Representative photographs are shown, together with mouse GAPDH levels as an internal control. Quantification of the intensity of the immunoreactive bands of both LC3-I and LC3-II, expressed in arbitrary units, was carried out using NIH Image J software. Results of densitometric analysis of immunoblots of LC3 in islets were expressed as the ratio of LC3-II to LC3-I. Data are mean ± SD of three independent experiments. *$p < 0.05$, versus control islet; $^{+}p < 0.05$, versus rapamycin-treated islets.

Results

In vitro *overinduction of autophagy in pancreatic islets by rapamycin*

Control islets, including untreated islets and 3-MA-treated islets, showed similar levels of endogenous expression of LC3-II protein (Figure 1). Islets treated with 1 or 10 ng/mL of rapamycin showed the highest expression of LC3-II protein. The conversion of LC3-I (cytosolic form) to LC3-II (membrane-bound lapidated form) was detected by immunoblotting. The amounts of LC3-II protein were three- to fivefold higher in 1 and 10 ng/mL rapamycin-treated islets, respectively, as assessed by the LC3-II/LC3-I ratio (Figure 1). The rapamycin-induced increase in LC3-II level suggests increased autophagy flux. Quantification of LC3-II band intensities showed that blockade of autophagy by 3-MA prevented the accumulation of LC3-II protein in islets treated with 1 or 10 ng/mL of rapamycin. With regard

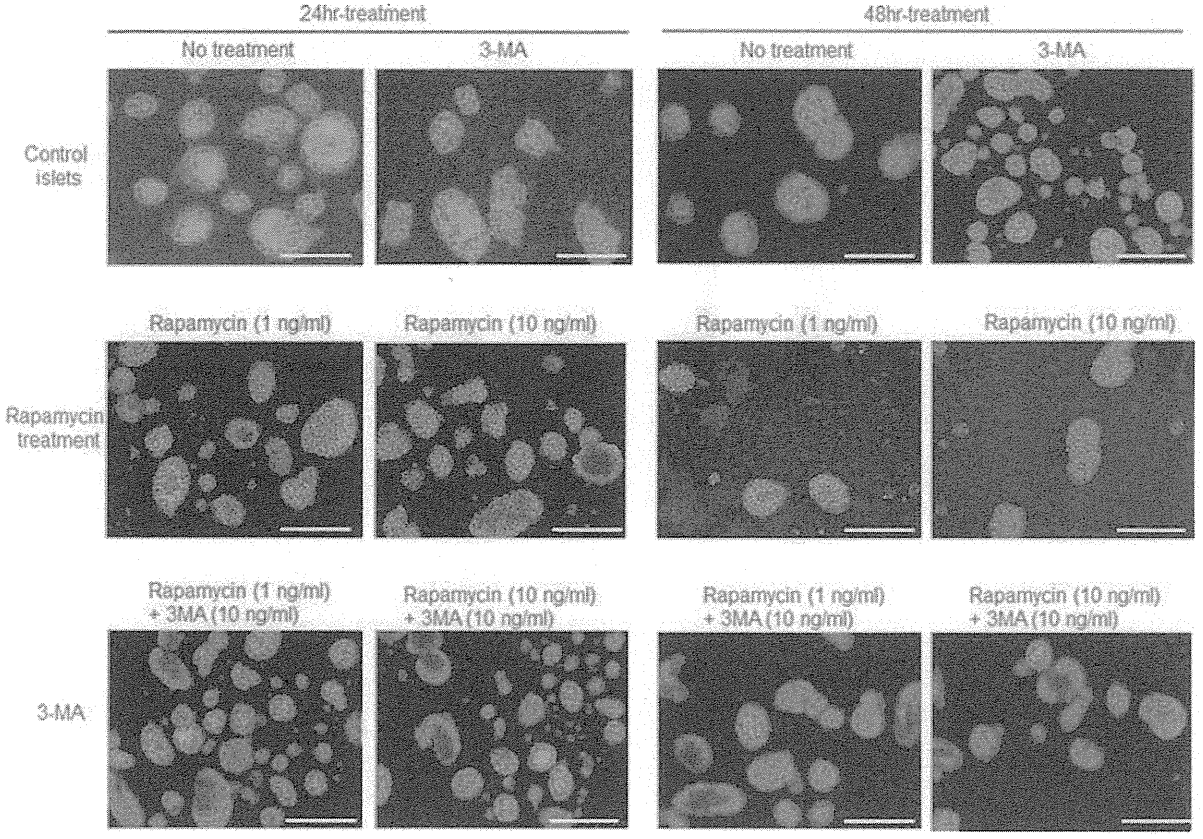

Figure 2: *In vitro* overinduction of autophagy in response to rapamycin treatment. Fresh islets samples were prepared from GFP-LC3 transgenic mice, and then incubated for either 24 or 48 h in the absence or presence of rapamycin. In 3-MA blocking, fresh islets were incubated in the presence of both rapamycin and 3-MA. After treatment, the GFP signal was detected by fluorescence microscopy. Bars = 100 μm.

to the conversion of LC3-I to LC3-II, the LC3-II/LC3-I ratio was significantly reduced in islets treated with rapamycin-plus-10 mM 3-MA compared with that of islets treated with rapamycin alone (Figure 1).

As shown in the top panels of Figure 2, a diffuse GFP-LC3 signal was detected in the control islets, with few GFP puncture dots. After 24 h incubation with 1 or 10 ng/mL of rapamycin, the number of GFP-LC3 dots was markedly increased; most dots were detected as cup- or ring-shaped structures (left middle panels, Figure 2). These findings indicate overinduction of autophagy in rapamycin-treated islets. In contrast, the fluorescence level of GFP-LC3 signal in rapamycin-treated islets in the presence of 10 mM 3-MA was diffuse and returned to the basal level of autophagy in control islets (left bottom panels, Figure 2). After 48 h incubation with rapamycin, many large ring- or cup-shaped structures were identified by fluorescence microscopy (right middle panels, Figure 2). Furthermore, the fluorescence signals of GFP-LC3 in rapamycin-plus-3-MA-treated islets continued to show diffuse distribution and persisted at the basal level of autophagy seen in the control islets (right bottom panels, Figure 2). Taken together, the results indicate that the blocking effects of 3-MA were persistent rather than transient.

Rapamycin-related overinduction of autophagy in islet cells reduces islet viability

To examine the effect of overinduction of autophagy by rapamycin on islet viability, we performed MTS assay (Figure 3) and fluorescence labeling with TMRE and 7-AAD (Figure 4). Viability under treatment with 3-MA alone was similar to the control islets (Figure 3). Treatment with 1 and 10 ng/mL rapamycin resulted in approximately 43% and 51% reduction of viability, respectively (Figure 3). In contrast, 3-MA ameliorated the effect of rapamycin on islet viability (Figure 3).

To further determine the effect of rapamycin on islet viability, islet cells were stained with TMRE or 7-AAD and assessed by FACS analysis. 3-MA had no significant effect on islet viability (control, 80.5 ± 4.5%; 3-MA, 80.4 ± 5.5%) and the percentages of dead cells (i.e. 7-AAD-positive cells; control, 4.7 ± 3.5%; 3-MA, 3.9 ± 4.3%). Rapamycin significantly decreased the proportion of TMRE-positive cells

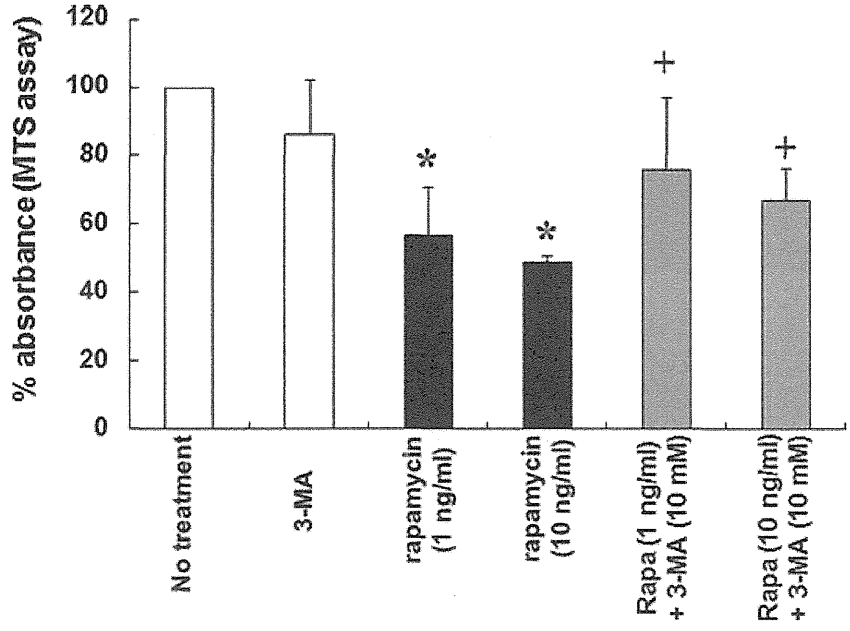

Figure 3: *In vitro* viability assessments of rapamycin-treated islet by MTS assay. Control islets, rapamycin-treated and rapamycin-3-MA-treated islets were assessed for islet viability. Data are mean ± SD of five independent islets preparations. The% absorbance of treated islets was expressed relative to absorbance of control islets, which was set at 100%. *$p < 0.05$, versus control islets; $^{+}p < 0.05$, versus rapamycin-treated islets.

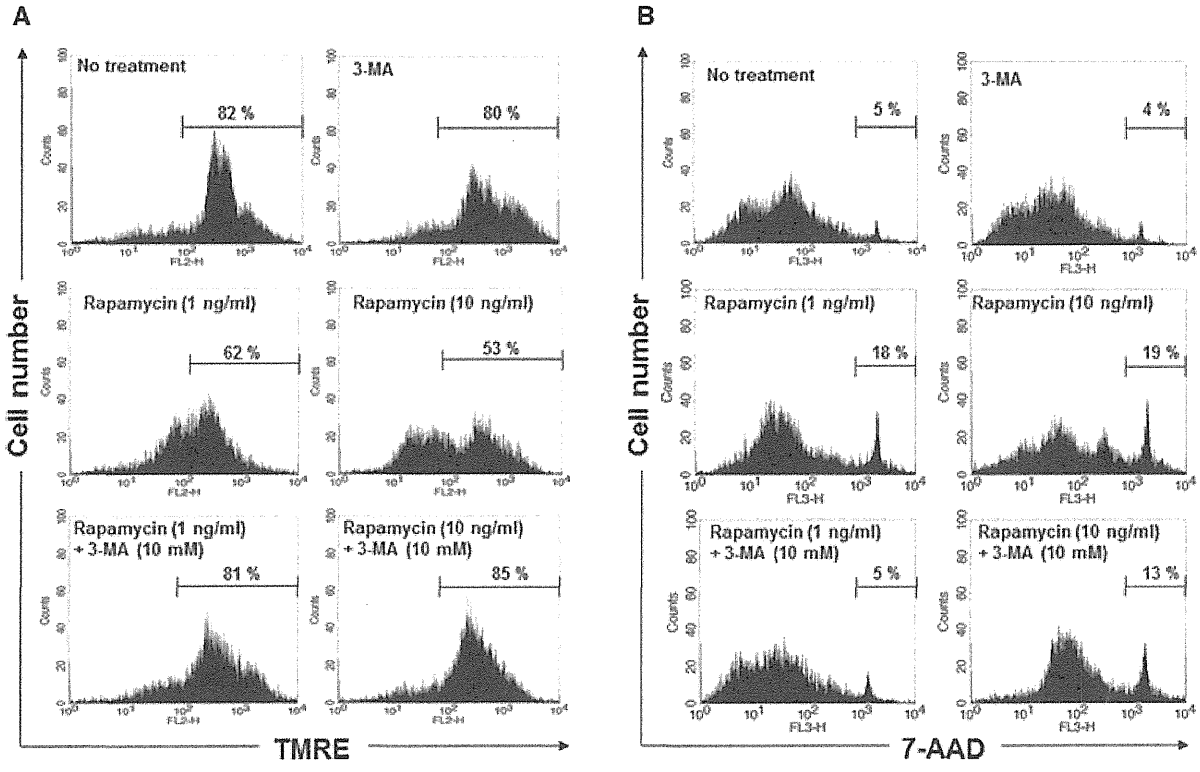

Figure 4: *In vitro* analysis of the cytotoxic effect of rapamycin and upregulation of autophagy. Islets were incubated with either 1 or 10 ng/mL of rapamycin for 24 h to overinduce autophagy. In blocking assay, islets were cultured with rapamycin in the presence of 10 mM 3-MA. After dispersion of mice islets into single cell suspensions, cells were stained with TMRE or 7-AAD. (A) Pancreatic β cells were analyzed for the relative percentage of apoptotic or nonapoptotic cells by TMRE. (B) Dead cells represented 7-AAD-positive cells. Data are representative of five independent experiments using different mice islets reparations.

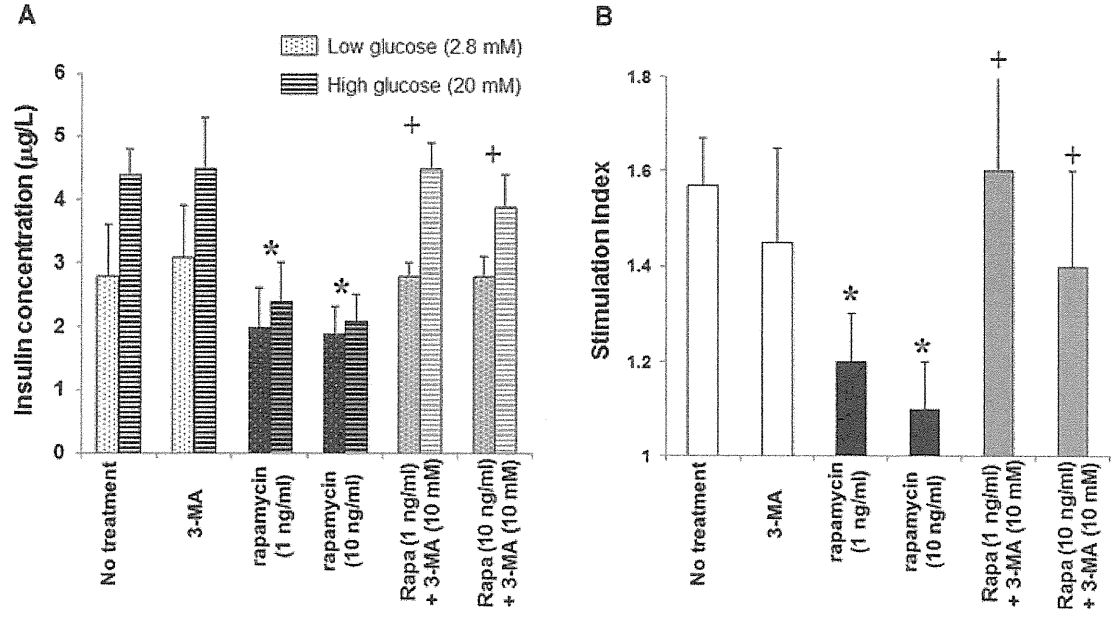

Figure 5: *In vitro* assessment of the effect of rapamycin on insulin production from islets. Production of insulin was assessed by static glucose challenge and the results expressed as both (A) blood insulin concentration and (B) stimulation index (SI). Data are mean ± SD of five independent islet preparations. *$p < 0.05$, compared with the control; $^{+}p < 0.05$, compared with rapamycin alone.

(1 ng/mL of rapamycin, 62.4 ± 6.7%; 10 ng/mL of rapamycin, 52.1 ± 6.1%; compared with the control, $p < 0.05$), and significantly increased the percentage of 7-AAD-positive cells (1 ng/mL of rapamycin, 17.7 ± 7.6%; 10 ng/mL of rapamycin, 18.7 ± 6.7%; compared with the control islets, $p < 0.05$). The addition of 3-MA to rapamycin-treated islets ameliorated the effects of the latter on the percentages of both viable and dead cells (Figures 4A and B). Taken together, these data suggest that rapamycin-induced overinduction of autophagy negatively affects islet viability and mitochondrial integrity, and that these effects are blocked by 3-MA.

Rapamycin reduces islet insulin production

Islet insulin potency was assessed by static glucose challenge *in vitro*. In control islets, insulin was secreted at 4.4–4.5 μg/L under high glucose medium (Figure 5A). In contrast, insulin secretion under high glucose medium was significantly inhibited in rapamycin-treated islets and treatment with rapamycin elicited approximately 45–53% reduction in insulin concentration (Figure 5A). We also analyzed islets' insulin production using the SI. The SI of untreated control islets was 1.57 ± 0.13 (Figure 5B). 3-MA did not have a significant effect on insulin production compared with the control islets. However, rapamycin significantly reduced the SI (1 ng/mL of rapamycin, 1.20 ± 0.1; 10 ng/mL of rapamycin, 1.11 ± 0.12; $p < 0.05$, each, compared with the control islets). The addition of 3-MA to rapamycin-treated islets markedly improved both insulin production and SI. Especially, insulin production showed complete recovery in islet treated with 1 ng/mL of rapamycin and 10 mM of 3-MA (Figures 5A and B). These results indicate that rapamycin elicits not only overinduction of autophagy but also reduction of both islet viability and *in vitro* insulin function.

Effect of nutrient starvation on autophagy in GFP-LC3 transgenic mice

To confirm the beneficial effects of 3-MA on induction of autophagy in the intact animal, we used GFP-LC3 transgenic mice and examined autophagy in 3-MA-treated transgenic mice under starvation. In the control GFP-LC3 transgenic mice, few GFP-LC3 dots were observed in pancreatic acinar cells and such dots were relatively small. In the pancreatic islets, no GFP dots were detected and these islets were clearly stained for insulin (top panels, Figure 6). The GFP-LC3 structures appeared 24 h after starvation as large cup-shaped structures in both islet and acinar cells. To validate these findings, we examined both muscle (as an example of nonessential tissue) and brain (as an essential tissue) tissues by fluorescence microscopy. As shown in Figure 7(A), no GFP dots were observed in the extensor digitorum longus muscles before starvation, however, GFP-LC3 dots appeared after 24 h starvation in muscle tissues (Figure 7B). On the other hand, in brain samples, including the cerebral cortex and medulla oblongata, no GFP-LC3 structures could be detected in spite of 24 h starvation (Figures 7D and F). In addition, islets starved for 24 h stained faintly for insulin (middle panels, Figure 6). The mean insulin staining intensity of starved islets was markedly reduced compared with that of untreated control islets, although the difference in insulin intensity was

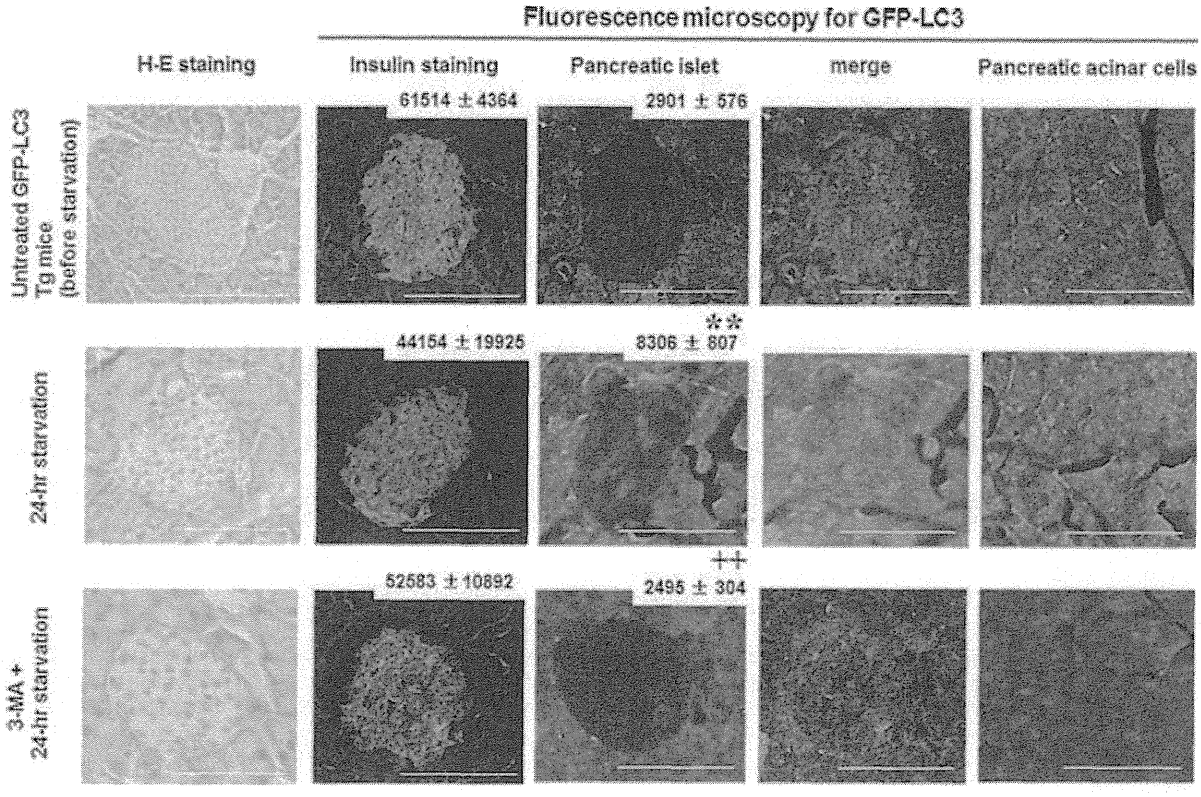

Figure 6: Starvation induced autophagy in pancreatic islets and acinar cells of GFP-LC3 transgenic mice. Representative images of islets stained with H&E and for insulin after 24 h starvation. Representative GFP images of pancreatic islets, acinar cells and merged *microphotographs of GFP images and insulin staining. Numbers in the right upper corner of the photographs represent the mean ± SD* intensity of GFP and insulin staining, expressed in arbitrary units, of five different islets. $^{**}p < 0.01$, compared with the control; $^{++}p < 0.01$, compared with 24 h starvation. Bars = 100 μm.

not significant (control, 61 514 ± 4364; starvation, 44 154 ± 19 925). The mean fluorescence intensity of GFP-dots was significantly higher in starved islets than untreated control islets (control, 2901 ± 576; starvation, 8306 ± 807; $p < 0.01$). The merged images of GFP signals of LC3 dots and the adjacent islets stained for insulin are shown in Figure 6. The merged microphotographs also showed weaker insulin intensity in starved islets compared with the control islets. The use of 3-MA during 24 h starvation ameliorated the effect of 24 h starvation as evident by the appearance—diffuse and few fluorescence signals of GFP-LC3 dots—and by the return of GFP fluorescence intensity in islets. Furthermore, the recovered islets stained positive for insulin and the intensity of such staining was similar to the control islets, as judged by both the mean staining intensity and the merged microphotographs (lower panels, Figure 6).

Effect of rapamycin on autophagy in GFP-LC3 transgenic mice

Finally, we assessed the effects of rapamycin on autophagy and insulin production in transgenic mice *in vivo*. For this purpose, the mice were treated with 0.2 mg/kg of rapamycin intraperitoneally daily for 1, 2, 3, 4 or 5 weeks. After 1 week of such treatment, small but few dots appeared in both islets and acinar cells, however, no significant difference was observed in the pancreas of rapamycin-treated mice and rapamycin-plus-3-MA (10 mM)-treated mice (top panels, Figures 8A and B). After 2, 3, 4 and 5 weeks of rapamycin treatment, a marked increase in the density of GFP-LC3 dots was observed and these dots appeared as ring- or cup-shaped structures in both islets and acinar cells (Figures 8A and B). The GFP fluorescence intensity was higher in 1-week treated islets than in untreated control islets, although no significant large GFP dots were observed (Figures 6 and 8A). After 2, 3, 4 and 5 weeks of treatment, the GFP fluorescence intensity in the treated islets was significantly up-regulated compared with those in control and 1-week treated islets. In spite of overinduction of autophagy in rapamycin-treated islets, the mean intensities of insulin in 2-, 3-, 4- and 5-week rapamycin-treated islets were significantly lower than the control untreated islets (Figure 8A). Interestingly, 3-MA ameliorated the changes in immunofluorescence, including GFP-LC3 dots and insulin staining intensity, which reflects rapamycin-induced overinduction of autophagy (Figure 8B). The merged

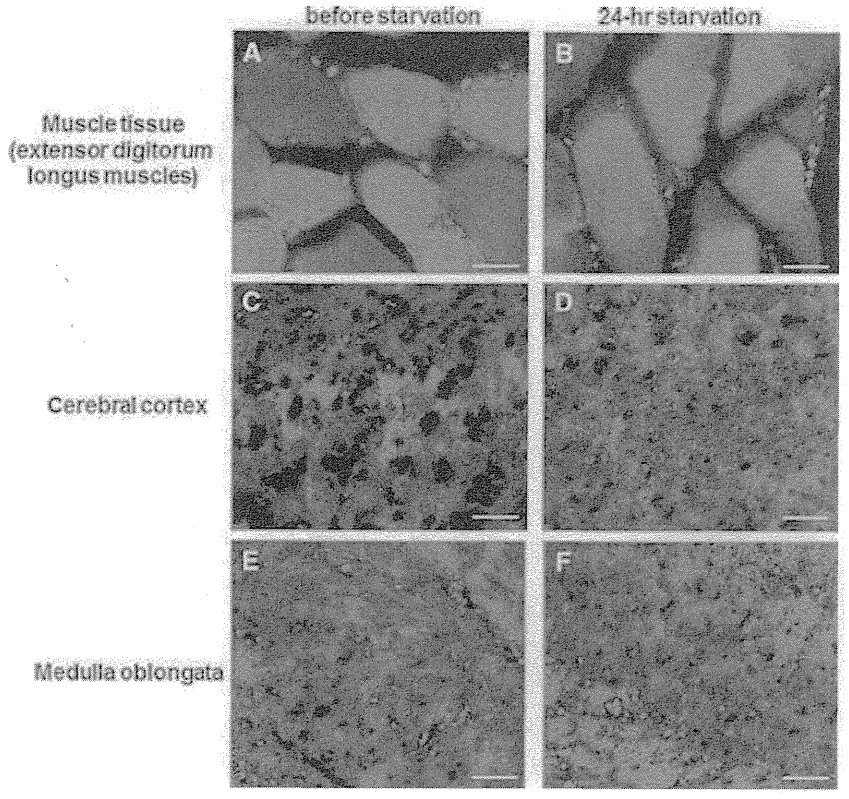

Figure 7: Starvation induced autophagy in muscle tissues, but not in brain. GFP images of transverse sections of extensor digitorum longus muscle (A) before starvation and (B) after starvation. GFP images of the cerebral cortex (C) before starvation and (D) after starvation. GFP images of medulla oblongata (E) before starvation and (F) after starvation. Bars = 10 μm.

microphotographs also demonstrated reduced insulin intensity in rapamycin-treated islets and that the degenerative change showed significant recovery in islets of the rapamycin-plus-3-MA group. TUNEL-positive cells were detected in 2-, 3-, 4- and 5-week rapamycin treated islets. In contrast, no such cells were observed in islets treated with rapamycin-plus-3-MA. Taken together, these *in vivo* findings correlated well with the *in vitro* data, including islet insulin potency and TMRE viability assay.

To further determine the effects of rapamycin on islet function in mice, we measured nonfasting blood glucose and plasma insulin concentrations. Rapamycin had no significant effect on nonfasting blood glucose levels, and near-normoglycemia was noted in mice treated with rapamycin alone and in those treated with rapamycin-plus-3-MA (Figures 9A and B). At days 14, 21, 28 and 35 after treatment, plasma insulin levels were higher in rapamycin-plus-3-MA-treated mice than in rapamycin-treated mice. Especially, plasma insulin concentration at day 14 in rapamycin-treated mice was significantly lower than in rapamycin-plus-3-MA-treated mice (Figures 9C and D). All other differences in insulin concentration were not significant between the two groups. Interestingly, in IPGTT performed at day 14, the blood glucose level of mice treated with rapamycin alone was significantly higher than in those treated with rapamycin-plus-3-MA at 15, 30, 60, 90 and 120 min after injection of glucose. Thus, rapamycin elicited a diabetic glucose pattern in mice (Figure 9E). In contrast, in the same test performed at day 28, the blood glucose levels of rapamycin-treated mice were similar to those of mice treated with rapamycin-plus-3-MA, and the pattern of blood glucose after injection was also similar between the two groups (Figure 9F). Taken together, rapamycin treatment resulted in impairment of *in vivo* glucose tolerance until 2 weeks after treatment and this abnormality was reversed by co-administration of 3-MA. It is possible that this abnormality of glucose tolerance represents physiological adjustment, such as reduction of insulin resistance at day 28. Further analysis of this phenomenon requires *in vivo* experiments of long-term rapamycin treatment.

Discussion

Rapamycin has deleterious effects on islet β cell based on the blockade of VEGF-mediated survival pathways and inhibition of β-cell proliferation and by induction of apoptosis (20,34,42). Accordingly, we raised the question of whether rapamycin in islet transplantation is a friend or a foe. In this study, we focused on the effect of rapamycin on autophagy and evaluated the direct effect of rapamycin on islet β cells. Using various techniques, the results demonstrated for the first time that rapamycin at therapeutically used concentrations, overinduced autophagy both *in vitro* and *in vivo* and that this effect on islet β cells impaired both islet viability and insulin potency.